

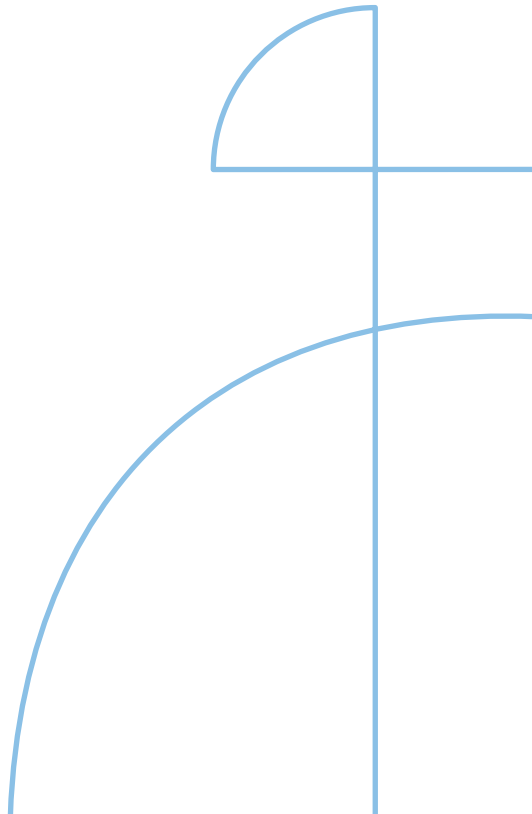


Doctoral Thesis in Vehicle and Maritime Engineering

# **Intrinsic Self-Sensing in Advanced Composites Enabled by Carbon Nanostructures**

**TOBIAS KARLSSON**

KTH ROYAL INSTITUTE OF TECHNOLOGY



# **Intrinsic Self-Sensing in Advanced Composites Enabled by Carbon Nanostructures**

**TOBIAS KARLSSON**

Academic Dissertation which, with due permission of the KTH Royal Institute of Technology, is submitted for public defence for the Degree of Doctor of Philosophy on Tuesday the 5th of May 2026, at 10:00 a.m. in F3, Lindstedtvägen 26, Stockholm.

Doctoral Thesis in Vehicle and Maritime Engineering  
KTH Royal Institute of Technology  
Stockholm, Sweden 2026

© Tobias Karlsson

TRITA-SCI-FOU 2026:05  
ISBN 978-91-8106-551-0

Printed by: Universitetservice US-AB, Sweden 2026

# Abstract

Lightweight composite structures have become essential in modern aerospace engineering, where increasing demands for fuel efficiency, reduced emissions, and improved operational reliability place new requirements on both materials and manufacturing. As composite components grow more advanced, featuring co-cured components, complex geometries, and thinner design margins, the need for improved insight into their internal behaviour becomes critical. Existing sensing technologies struggle to provide local, *in-situ* information from the composite's interior during manufacturing or throughout its service life, without compromising structural integrity. This creates a gap between the capability of current sensing approaches and the monitoring demands required by the complexity of next-generation composites.

This thesis addresses this gap by investigating the feasibility of embedding nanomaterial-based sensing structures, primarily vertically aligned carbon nanotube (VACNT) forests, into fibre-reinforced polymer composites. The overarching aim is to explore how such sensors can be integrated with minimal structural intrusion, from where their sensing behaviour originates, and how they can provide reliable, multifunctional monitoring both during manufacturing and in the cured state. The work spans the development of embedding and contacting strategies, bottom-up characterisation to investigate sensing mechanisms, and the exploration of both direct current (DC) and alternating current (AC) measurement approaches. Collectively, the research seeks to expand the understanding of how nanomaterial sensors interact with composite materials and how they can support the design of future multifunctional aerospace structures.

The findings demonstrate that VACNT forests can be embedded into composite laminates without compromising the composite's mechanical structure, while providing robust and reproducible sensing capabilities. A bottom-up analysis helps determine that the embedded VACNT forests' thermoresistive behaviour is governed by fluctuation-assisted tunnelling, and their linear piezoresistive response originates in the intrinsic piezoresistivity of individual CNTs. The VACNT forests enable local *in-situ* cure monitoring of prepreg laminate, detecting key process transitions. Strategies for sensing in conductive carbon fibre environments are established, as well as comparisons with alternative nanomaterial-based sensors such as graphene coatings. Finally, by transitioning from DC resistance to AC impedance measurements, the work shows that embedded CNT structures can detect high transverse pressures and exhibit frequency-dependent sensing sensitivity.

Together, these results establish VACNT forests as a promising, multifunctional, and structurally compatible sensing concept for advanced composite structures, offering new pathways for embedded process monitoring, structural health monitoring, and the development of next-generation multifunctional aerospace components.

**Keywords**

Embedded Sensing, Cure Monitoring, Structural Health Monitoring, Vertically Aligned Carbon Nanotubes, Resistive Sensing, Impedance Spectroscopy

# Sammanfattning

Lätta kompositstrukturer har blivit avgörande inom modern flygteknik, där ökade krav på bränsleeffektivitet, minskade utsläpp och förbättrad driftsäkerhet ställer nya krav på både material och tillverkningsprocesser. I takt med att kompositkomponenter blir allt mer avancerade, med samhärdade komponenter, komplexa geometrier och tunnare konstruktionsmarginaler, blir behovet av förbättrad insyn i deras interna beteende allt mer kritiskt. Befintlig sensorteknologi har svårt att ge lokal, *in-situ* information från kompositens inre under tillverkning samt under dess livslängd, utan att kompromissa med den strukturella integriteten. Detta skapar ett gap mellan förmågan hos nuvarande sensorlösningar och de övervakningskrav som uppkommer i och med nästa generations komplexa kompositstrukturer.

Denna avhandling adresserar detta gap genom att undersöka möjligheten att integrera nanomaterialbaserade sensorstrukturer, främst vertikalt riktade kolnanorörsskogar (VACNT), i fiberförstärkta polymerkompositer. Det övergripande målet är att utforska hur sådana sensorer kan integreras med minimal strukturell påverkan, varifrån deras sensorbeteende har sitt ursprung, och hur de kan erbjuda tillförlitlig och multifunktionell övervakning både under tillverkning och i det härdade tillståndet. Arbetet omfattar utveckling av strategier för integrering och elektrisk kontaktering av sensorn, bottom-up-karakterisering för att undersöka sensormekanismer, samt utforskning av mätmetoder baserade på både likström (DC) och växelström (AC). Övergripande syftar forskningen till att utvidga och öka förståelsen för hur nanomaterialbaserade sensorer interagerar med kompositmaterial och hur de kan stödja utvecklingen av framtida multifunktionella flygstrukturer.

Resultaten visar att VACNT-skogar kan integreras in i kompositlaminat utan att påverka laminatet negativt mekaniskt, samtidigt som de erbjuder robusta och reproducerbara sensorfunktioner. En bottom-up-analys fastställer att de inbäddade VACNT-skogarnas termoresistiva beteende styrs av fluktuationsassisterad tunnling, och att dess linjära piezoresistiva beteende härrör från den piezoresistiva effekten hos enskilda kolnanorör. VACNT-skogarna möjliggör lokal *in-situ* övervakning av härdningsprocessen i prepreglaminat, där betydande processövergångar kan övervakas. Strategier för mätningar i konduktiva kolfibermiljöer etableras, liksom jämförelser med alternativa nanomaterialbaserade sensorer såsom ytbeläggningar av grafen. Slutligen visar övergången från DC-resistans till AC-impedansmätningar att de inbäddade CNT-strukturerna kan detektera höga transversella tryck och uppvisa frekvensberoende sensorkänslighet.

Sammanfattningsvis etablerar dessa resultat VACNT-skogar som ett lovande, multifunktionellt och strukturellt kompatibelt sensorkoncept för avancerade kompositstrukturer, som erbjuder nya möjligheter för inbäddad processövervakning, strukturell hälsoövervakning och utveckling av nästa generations multifunktionella flygkomponenter.

### **Nyckelord**

Inbyggd sorteknik, Härdningsövervakning, Strukturell hälsoövervakning, Vertikalt riktade kolnanorör, Resistiv mätning, Impedansspektroskopi.

# Acknowledgments

This doctoral thesis has been carried out at the Division of Material and Structural Mechanics, Department of Engineering Mechanics, KTH Royal Institute of Technology, Stockholm, Sweden. The work has been funded by the Swedish Governmental Agency for Innovation Systems, Vinnova, through the IntDemo program, Strategic Innovation Program LIGHTer, LIGHTer Academy and Swedish National Aviation Engineering Research Program (NFFP) together with Saab AB, who are gratefully acknowledged.

I would like to sincerely thank my supervisor, Malin Åkermo. Your support and care have been deeply appreciated during these years, which have included many challenges. From the initial trials we did in the lab together, to the discussions and reviews leading up to the published papers. I will forever be thankful for your support and belief in me.

I would also like to express my sincere gratitude to my co-supervisor, Per Hallander. Your guidance and steady support have been invaluable throughout this work. From preparing samples together to discussions and curiosity about finding the next research topic and analysing data, you have been part of every step, all while delivering jokes with references I never quite managed to understand.

To all the fellow PhD students and post-docs in the department, I want to start by thanking Ross, Karl, Lynn, Gustav, Johan Larsson and Johan Nygren for the help and support I received when I first arrived at the department. Over the years, some of you completed your time at KTH while new colleagues joined our group. To the colleagues who joined later, Abhik, Alfredo, Gracieth, Helena, Junaid, Kaushik, Maria, Mehdi, Peter, and Sai, I have thoroughly enjoyed our

lunch conversations, some more serious than others, our lunch walks, celebrations, after works and all the time we have spent together! We began as colleagues, now, I am happy to call you my friends!

My sincere thanks go to the people in the department and, in particular, the Lightweight Structures group, for all the small conversations, ideas, support and words of encouragement in the corridors over these years. It has all contributed and helped me to arrive at this point.

A special thanks goes to Monica and Anders in the lab, whose patience and support with my work, which has not necessarily been tidy at all times, have been invaluable. You have always expressed curiosity about my work and helped me learn and improve in my experimental work. You are kind and helpful people, and I will always be grateful to you.

My gratitude extends to the master's thesis students I have supervised, Riccardo and Martin. Their contributions and enthusiasm for the research presented in this thesis have been greatly valued and have helped me realise my ideas experimentally.

Lastly, to my family. I will forever be thankful for the unconditional love and support I have received. To my grandparents, mother, father and brother, you have always been there, helping and motivating me through tougher times and celebrating my wins and accomplishments. I love you!

Tobias Karlsson

Stockholm, Mars 2026

# Dissertation

This doctoral thesis consists of an introduction to the area of research and the following appended papers:

## **Paper A**

Karlsson T, Hallander P, Liu F, Poot T, Åkermo M. *Sensing abilities of embedded vertically aligned carbon nanotube forests in structural composites: From nanoscale properties to mesoscale functionalities*. Compos B Eng 2023;255:110587.

<https://doi.org/10.1016/j.compositesb.2023.110587>

## **Paper B**

Karlsson T, Dutta A, Hallander P, Åkermo M. *In-situ cure monitoring of structural composite by embedment of vertically aligned carbon nanotube forests*. Compos B Eng 2025;293:112105.

<https://doi.org/10.1016/j.compositesb.2024.112105>

## **Paper C**

Karlsson T, Hallander P, Åkermo M. *Isolation strategies of carbon nanotubes for resistive sensing in carbon fibre prepreg laminates*. Proceedings of 21<sup>st</sup> European Conference on Composite Materials, July 2 – 5, 2024, Nantes, France.

**Paper D**

Karlsson T, Zhybak M, Hallander P, Åkermo M. *Comparative study of graphene coated glass fibers and carbon nanotube forests as embedded structural health monitoring systems*. Proceedings of 24<sup>th</sup> International Conference on Composite Materials, August 4 – 8, 2025; Baltimore, USA.

**Paper E**

Karlsson T, Janus P, Hallander P, Åkermo M (2026). *Sensing of Transverse Pressure in Structural Composite by Impedance Spectroscopy on Embedded Carbon Nanotube Sensing Structures*. (Accepted on 27<sup>th</sup> of March 2026 to journal “Advanced Composites and Hybrid Materials”).

**Conference paper not included in the thesis**

Karlsson T, Hallander P, Åkermo M. *Embedded carbon nanotubes for localized cure monitoring*. Proceeding of 20<sup>th</sup> European Conference on Composite Materials, June 26 – 30, 2022; Lausanne, Switzerland.

## List of Abbreviations

CNT	Carbon Nanotube
SWCNT	Single-Walled Carbon Nanotube
MWCNT	Multi-Walled Carbon Nanotube
VACNT	Vertically Aligned Carbon Nanotube
FRPC	Fibre-Reinforced Polymer Composite
GF	Glass Fibre
CF	Carbon Fibre
DC	Direct Current
AC	Alternating Current
SHM	Structural Health Monitoring
rGO	Reduced Graphene Oxide
VBO	Vacuum Bag Only
TEM	Transmission Electron Microscopy
SEM	Scanning Electron Microscopy
TGA	Thermal Gravimetric Analysis
CTE	Coefficient of Thermal Expansion
FAT	Fluctuation-Assisted Tunneling

VRH	Variable Range Hopping
NRC	Negative Resistance Coefficient
TCR	Temperature Resistance Coefficient
$T_g$	Glass Transition Temperature
RTM	Resin Transfer Moulding
VARTM	Vacuum-Assisted Resin Transfer Moulding
ATL	Automated Tape Lay
AFP	Automated Fibre Placement
CVD	Chemical Vapour Deposition
FBG	Fibre Bragg Grating

## Contributions to the Papers

The author's contributions to the appended papers area as follows:

**Paper A** – *Sensing abilities of embedded vertically aligned carbon nanotube forests in structural composites: From nanoscale properties to mesoscale functionalities*

T. Karlsson, P. Hallander and M. Åkermo conceptualised the idea and defined the methodology. T. Karlsson performed the experimental investigation. F. Liu performed the TEM study on individual CNTs and the SEM study of prepreg surfaces. T. Poot performed the SEM study on the as-grown VACNT forest. T. Karlsson analysed the data, wrote the original manuscript, and reviewed it jointly with P. Hallander and M. Åkermo. P. Hallander and M. Åkermo and supervised the work.

**Paper B** – *In-situ cure monitoring of structural composite by embedment of vertically aligned carbon nanotube forests*

T. Karlsson, A. Dutta, P. Hallander and M. Åkermo conceptualised the idea and defined the methodology. T. Karlsson performed the experimental investigation, with help from A. Dutta during the compaction experiments. T. Karlsson analysed the data, wrote the original manuscript, and reviewed it jointly with A. Dutta, P. Hallander and M. Åkermo. P. Hallander and M. Åkermo supervised the work.

**Paper C** – *Isolation strategies of carbon nanotubes for resistive sensing in carbon fibre prepreg laminates*

T. Karlsson, P. Hallander and M. Åkermo conceptualised the idea and defined the methodology. T. Karlsson performed the experimental investigation. T. Karlsson analysed the data, wrote the original manuscript, and reviewed it jointly with P. Hallander and M. Åkermo. P. Hallander and M. Åkermo and supervised the work.

**Paper D** – *Comparative study of graphene coated glass fibers and carbon nanotube forests as embedded structural health monitoring systems*

T. Karlsson, P. Hallander and M. Åkermo conceptualised the idea and defined the methodology. M. Zhybak provided the graphene-coated glass fibre weave. T. Karlsson performed the experimental investigation. T. Karlsson analysed the data, wrote the original manuscript, and reviewed it jointly with P. Hallander and M. Åkermo. P. Hallander and M. Åkermo and supervised the work.

**Paper E** – *Sensing of Transverse Pressure in Structural Composite by Impedance Spectroscopy on Embedded Carbon Nanotube Sensing Structures*

T. Karlsson, P. Hallander and M. Åkermo conceptualised the idea. T. Karlsson and P. Janus defined the methodology. T. Karlsson performed the experimental investigation. T. Karlsson and P. Janus analysed the data. T. Karlsson wrote the original manuscript, and reviewed it jointly with P. Janus, P. Hallander and M. Åkermo. P. Hallander and M. Åkermo supervised the work.

# CONTENTS

1	Introduction .....	1
1.1	Background.....	1
1.2	Aim and Scope of Work.....	5
2	Manufacturing of Composite Components .....	7
2.1	Forming.....	9
2.2	Curing.....	10
3	Nanomaterials for Embedded Sensing.....	13
3.1	Graphene and Carbon Nanotubes .....	13
3.2	Conductive Structures and Percolated Systems .....	15
3.3	Sensing Mechanisms .....	18
3.3.1	Production and Cure Monitoring .....	18
3.3.2	Structural Health Monitoring .....	20
3.3.3	Direct Current versus Alternating Current for Sensing.....	22
4	The VACNT Forests and Embedment into FRPCs.....	23
5	Comparison with Optical Methods for Embedded Sensing.....	27
5.1	Pre-study Benchmarking using FBGs .....	29
6	Summary of Papers .....	31
7	Contributions to the Field .....	37
8	Future Work .....	41
	References.....	43



# 1 Introduction

## 1.1 Background

Fibre-reinforced polymer composites (FRPCs) are increasingly employed in high-performance structural applications where minimising structural mass is critical, particularly in aerospace. Their adoption is primarily driven by their high specific stiffness and strength, which enable load-bearing components with substantially reduced weight compared with metallic alternatives. Due to their anisotropic nature, FRPCs also offer extensive design flexibility. This is achieved by adjusting fibre orientation, fibre volume fraction, stacking sequence, and the selection of fibre and matrix systems. Although complex, such design flexibility allows engineers to optimise the stiffness and strength of components, adapted to meet specific performance requirements.

For these reasons, the adoption of FRPCs has played a decisive role in reducing the structural weight of modern airliners. The Airbus A350 consists of approximately 53% composite materials by weight, and the Boeing 787 Dreamliner uses around 50%. In contrast, earlier aircraft such as the Boeing 767 incorporated only about 3% composites, relying primarily on aluminium, which constituted roughly 77% of its structural mass. The extensive integration of FRPCs in the A350 and 787 airframes has contributed to substantial improvements in fuel efficiency, with reported reductions of 20–22% compared with earlier-generation aircraft [1]. Reducing weight to achieve fuel savings is one of the reasons for the increased use of FRPCs.

FRPCs also have widespread use beyond aerospace, particularly in the energy and maritime sectors. In wind energy, glass-fibre composites are the dominant material for turbine blades due to their high specific strength and stiffness, low

weight, and inherent corrosion resistance. Similarly, glass-fibre composites have long been established in marine structures, where their superior fatigue performance and non-corrosive nature provide significantly longer service life compared with metallic hulls.

The examples above show how composites have found specialised roles in applications where their properties offer clear advantages to traditional metallic structures. However, continued weight savings in aerospace are increasingly more complex. A strategy to achieve continued weight savings is to design and co-cure more intricate components in an effort to reduce the number of parts needed to be joined together in assembly. The consequence of this, apart from cheaper and more efficient manufacturing, is the reduction in the number of fasteners required in assembly, the fasteners themselves constituting a very significant amount of weight. An example of this design philosophy is presented in Fig. 1, presenting an integral composite part where the stringers, rib feet and shell have been co-cured to reduce the number of fasteners.

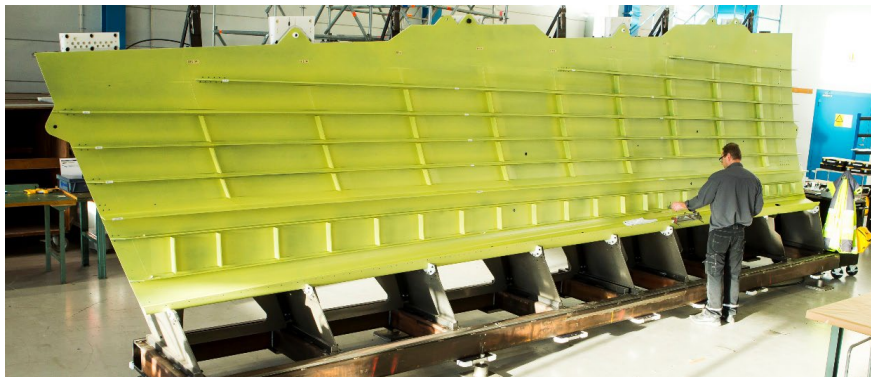


*Figure 1: Integral composite part with co-cured stringers and rib feet with the shell. From Clean Sky project, courtesy of Saab AB*

What has been discussed up to this point concerning weight has exclusively regarded the structural weight of the aircraft. However, an aircraft is more than its structural weight. The total weight of the aircraft consists of the weight of the mechanical structure, the airframe, and the systems operating the aircraft. This includes computers, radars, engines, and more. An example contrasting the different weights is given in Fig. 2, where the airframe of the Gripen E from SAAB is approximately 37 % of the total weight, and 63 % consists of systems. This example illustrates that reducing structural weight alone has a limited impact on the overall aircraft weight. This relation is not the same for civilian aircraft, where about 50 % of the total weight is the structural airframe weight

when unloaded. To achieve further weight savings, one approach is to rethink the design of systems in an effort to fit more functions into the airframe in parallel with its pure mechanical function, achieving multifunctionality.

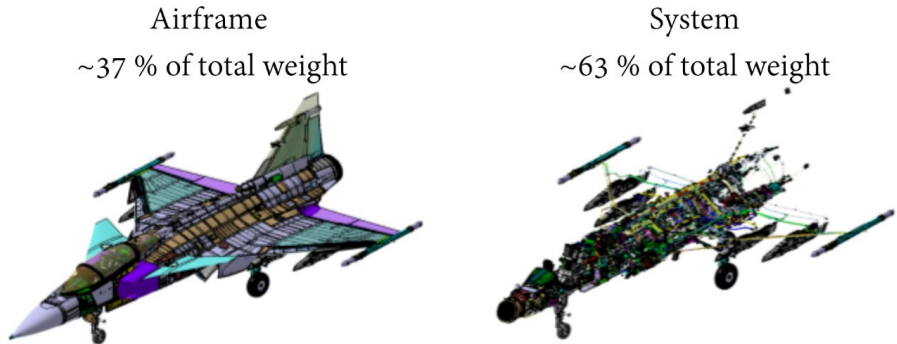


Figure 2: Comparison of airframe and system weights to the total weight of a Gripen E. Courtesy of Saab AB

Multifunctionality of composite structures is defined by having more than one functionality, adding to the mechanical functionality. Some examples, such as radar transparency, are a matter of material selection, choosing to manufacture randoms by glass fibre rather than conductive carbon fibres, to achieve transparency. This is an example of a passive multifunctional structure, which can also include lightning strike protection and anti-icing surfaces, for example. Active multifunctionality in composite structures is also a topic, which can include morphing structures [2], de-icing solutions [3,4], structural batteries [5–8], and embedded sensing strategies [9,10].

The examples above illustrate that multifunctionality in composite structures can encompass a wide range of added functionalities. In this thesis, embedded sensing refers to sensor elements or sensing structures that are integrated within the composite material itself, rather than applied externally as surface-mounted devices. The purpose of embedding the sensor is to obtain *in-situ* measurements, capturing information from within the material volume and thereby enabling monitoring capabilities not achievable with surface-based techniques. This includes sensing during the manufacturing of thermosetting matrix systems as well as during the operational life of the component, where structural health monitoring (SHM) is performed.

Although embedded sensing does not directly reduce the structural weight of an airframe, it may offer several long-term benefits. First, during the design of composite structures, safety factors and knock-down factors are applied to

account for uncertainties in material behaviour. Improved insight from SHM could, over time, enable a refinement of these design factors by providing a more accurate understanding of in-service performance, ultimately allowing for lighter structural designs. Second, embedded sensing has the potential to significantly reduce maintenance costs. Approximately 90% of maintenance time is spent disassembling components to reach inspection points and subsequently reassembling them. By enabling condition-based (directed) maintenance rather than scheduled maintenance, SHM systems could reduce both time and cost. Third, efforts to reduce weight increasingly rely on more advanced and co-cured components. These new complex geometries introduce new challenges for inspection and require sensors to monitor them.

Embedded sensing in composite structures is the central theme of this thesis. Numerous sensing approaches have been reported in the literature, including optical, resistive, dielectric, and nanomaterial-based methods. When designing a sensor for embedment into the composite structure, the size of the sensor is critical in order to not interfere with, or deteriorate, the mechanical structure.

In this thesis, nanomaterial-based sensing structures have been the primary focus, while optical fibres were evaluated in an initial pre-study for benchmarking purposes. Consequently, the discussion of embedded sensing in FRPCs throughout this thesis concentrates mainly on nanomaterials (Chapter 3), with optical methods considered as a secondary method (Chapter 5).

## 1.2 Aim and Scope of Work

The aim of this work is to investigate the feasibility and performance of embedded sensing in structural composites using VACNT forests and related nanomaterial-based sensing structures. The overall objective is to understand how such nanomaterial structures can be embedded into fibre-reinforced polymer composites to enable reliable, multifunctional sensing throughout both its manufacturing and later continue during its operational life.

The scope of the thesis encompasses five interconnected research themes:

1. **Embedding, characterisation and sensor functionalities of VACNT forests**  
Developing methods to embed VACNT forests into prepreg-based composite laminates without compromising structural integrity and determine the origin of their sensing behaviour in the cured state through a bottom-up characterisation of the forests at the nano-, micro-, and mesoscales.
2. ***In-situ* cure monitoring**  
Evaluating the capability of embedded VACNT forests to resistively monitor events and processes during curing of thermosetting matrix and prepreg laminates.
3. **Resistive sensing in conductive carbon-fibre environment**  
Investigating strategies to electrically isolate embedded VACNT forests from surrounding conductive carbon fibre environment to enable reliable resistive measurements.
4. **Exploration of alternative conductive nanomaterials**  
Broadening the sensing concept by assessing other nanomaterials and structures – such as graphene coatings – and comparing their behaviours with VACNT-based sensors.
5. **Transition from DC to AC-based sensing**  
Studying impedance-based measurement strategies to investigate additional sensing capabilities of VACNT forests, exploring their dielectric properties and the influence of measurement frequency on both resistive and dielectric properties to explore their potential for multi-parameter sensing.

Together, these efforts aim to clarify how embedded nanomaterial sensors can be designed, implemented, and optimised for monitoring during manufacturing and for SHM throughout the operational life of advanced composite structures.



## 2 Manufacturing of Composite Components

Composite materials, by definition, consist of two or more distinct constituent materials to create a new material. Here, FRPCs are studied in application for lightweight structures. FRPCs, as the name implies, consist of fibres and polymers, where the fibres are the load-bearing component of the material, whilst the polymer fixes the fibres and transfers mechanical load onto them. Polymers can be divided into two groups, which are thermoplastic and thermosetting polymers. Thermoplastics are a group of polymers with the common property that the polymer chains are held together by intermolecular forces, such as van der Waals and hydrogen bonding, which weaken in strength as the polymer is heated. Consequently, thermoplastics become viscous and formable, and solidify again when the temperature is lowered, as the intermolecular forces increase in magnitude. This is different to thermosetting polymers, where, during the curing process, irreversible chemical bonds are formed, creating an insoluble network of interlinked polymers. Due to the chemical nature of thermosets, they are set in their shape once cured. In aerospace, thermosetting polymers are dominantly used today, although an increased interest has appeared in thermoplastics for speed and cost of manufacturing and recycling purposes. The thermoset industry standard in aerospace is epoxy for structural composites, although bismaleimides (BMI) are used for higher temperature applications.

The reinforcement in FRPCs consists of fibres. The most common ones in aerospace are carbon fibres (CF), glass fibres (GF), and aramid fibres (such as Kevlar). In this work, glass fibres are mostly used due to their non-conductive (electrical) nature. However, in structural composites in aerospace, carbon fibres are favoured due to their higher specific mechanical strength and

modulus. Continuous fibres are used for structural composites. To arrange the fibres in FRPCs, they can be unidirectional, in weaves of different patterns (plain, twill, satin), spread tows and non-crimp fabrics.

There are two avenues to manufacture FRPCs. The first uses dry fibres and impregnates the fibres with matrix during the manufacturing of the component. Processes using this avenue are traditional hand lay-up, resin transfer moulding (RTM), vacuum-assisted resin transfer moulding (VARTM), and vacuum-infusion moulding. The second avenue uses prepregs. Prepregs are plies of fibres in the form of weaves or unidirectional fibres pre-impregnated with matrix prior to manufacturing of the component. For this reason, prepregs need to be stored in a freezer, below the glass transition temperature ( $T_g$ ) of the uncured prepregs, reducing the reactivity of the pre-blended matrix. The most prevalent method in the aerospace sector to produce FRPCs is prepreg technology. It starts with the lay-up of the prepregs on a flat surface according to the design of the laminate, which can be performed by hand or automated with an automated tape lay (ATL) or automated fibre placement (AFP). Thereafter, the laminate is pre-consolidated under vacuum to evacuate air, if the lay-up was performed by hand. The automated processes roll the prepregs after lay-up, therefore not requiring pre-consolidation.

If a flat laminate is desired, the laminate is placed on a flat substrate, and a vacuum bag (including breather and peel ply or release film) is constructed around the laminate to apply vacuum pressure during the curing in order to evacuate remaining air during the cure cycle. Traditionally, resin-saturated prepregs have been the material of choice in the aerospace industry, relying on processing with elevated temperatures and pressures to collapse voids and evacuate entrapped air during the cure cycle. In recent years, however, vacuum-bag-only (VBO) prepreg systems have emerged as an alternative, requiring only vacuum pressure and heat in order to reduce manufacturing costs and energy consumption. Unlike conventional resin-saturated prepregs, VBO prepregs rely more on specifically engineered air-evacuation channels (see Fig. 3) to remove air from the laminate. These pathways remain open during the early stages of heating and are subsequently closed by resin flow at elevated temperatures, terminating the air-evacuation [11–15].

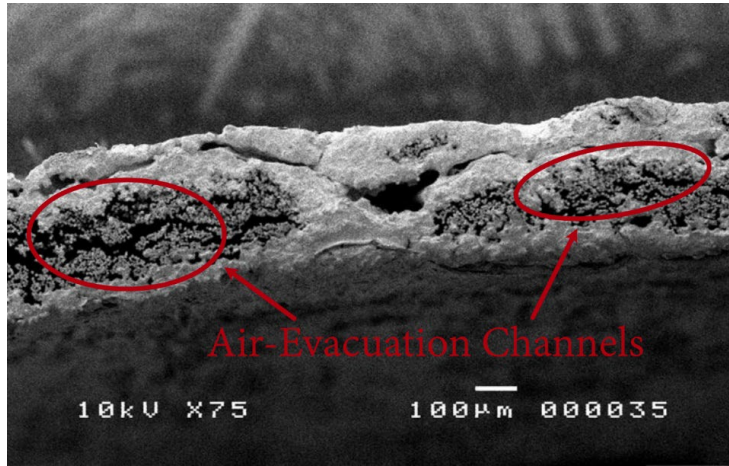


Figure 3: Air-evacuation channels in SEM, Courtesy of Sören Nilsson, Swerea Sicomp

## 2.1 Forming

Most components are not flat laminates and require forming of the laminate prior to cure. This can be done layer-by-layer by hand onto the curing tool, or by forming several plies thick laminates. The laminate can be formed using mechanical tooling or a flexible membrane and vacuum. Examples of simple profiles achieved with forming are shown below in Fig. 4.

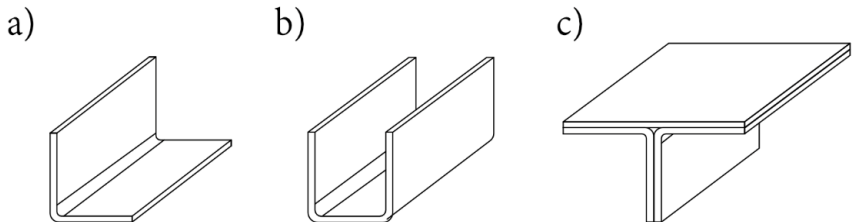


Figure 4: a) L-profile, b) U-profile, and c) T-profile

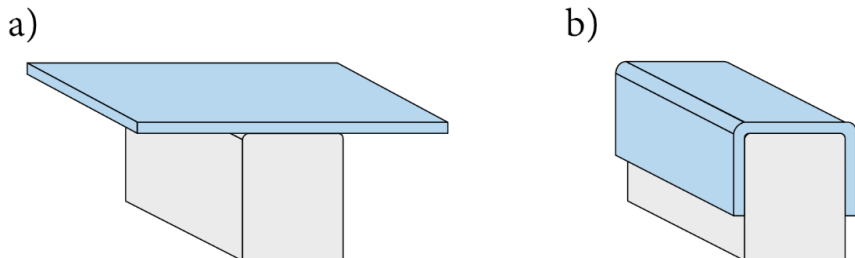


Figure 5: a) Flat laminate on forming tool prior to forming, b) Laminate on forming tool after forming

A commonly used forming method within the aerospace sector when manufacturing beams is hot-forming. Here, the laid-up flat laminate is heated up and formed onto a tool, see Fig. 5, using mechanical tooling or a flexible membrane and vacuum. Since the fibres cannot stretch, hot forming requires complex deformation both within individual plies and at their interfaces. Typically, controlled heating is essential to sufficiently reduce the resin viscosity and enable the necessary ply movement. Complex parts may require several layered up laminates and shells to be formed before being transferred to a cure tool, onto which the laminate is supported and bagged around during the cure cycle. An example of this is a standard T-section, see Fig. 5 C and Fig. 6, where two curvatures (L-profile) have been formed and later co-cured with a flat shell to form a T-profile.

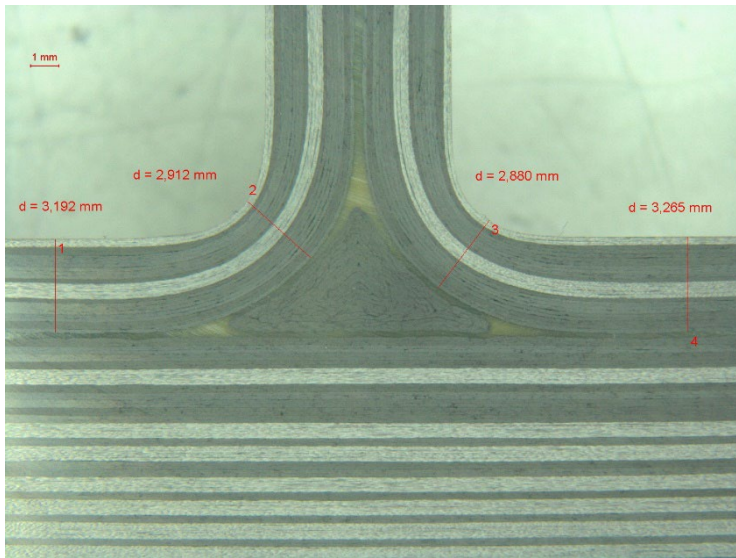


Figure 6: Micrograph of a co-cured T-profile cross-section, with a noodle. Courtesy of Saab AB

## 2.2 Curing

The cure of the thermosetting composite is performed in an autoclave or out-of-autoclave using a cure cycle, consisting of a temperature and a pressure cycle combined. The temperature cycle has three major phases, the ramp-up, a dwell at curing temperature, and a ramp-down. Two examples of cure cycles are shown in Fig. 7, using a curing temperature of 180°C. The temperature increases from room temperature up to the dwell at the curing temperature is called the ramp-up and must be carefully defined. The ramp-up is typically a few degrees

per minute, allowing for further compaction and consolidation of the laminate stacking to occur as the viscosity of the thermosetting matrix decreases, filling in the voids easier. If the ramp-up rate is too high, a loss of control of the exothermic reaction may occur, causing an uncontrolled increase in temperature causing damage to the component. Therefore, a ramp-up rate and schedule need to be carefully designed. For thicker components, it is common to use an intermediate dwell during the ramp-up, prior to reaching curing temperature, at an elevated temperature where the viscosity of the thermoset is low, allowing for the complete consolidation of the laminate before curing, see Fig. 7 cycle 2.

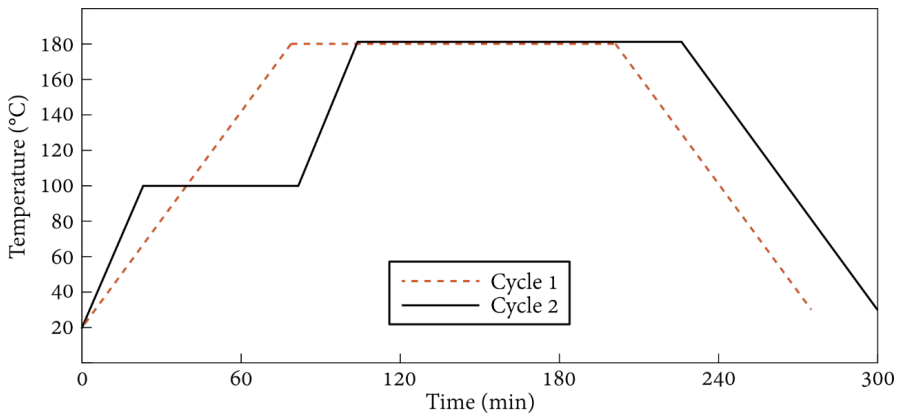


Figure 7: Two cure cycles with and without an intermediate dwell

Approaching the dwell at curing temperature, the curing of the thermoset initiates at a specific temperature, the hardener being activated thermally. As the cure continues, the degree of cure increases as the polymer network becomes increasingly cross-linked. Eventually, the gel-point is reached, from where the polymer network is cross-linked enough in order to not be soluble. From the gel-point, the matrix is able to carry mechanical load. The time at the curing temperature dwell lasts a few hours, depending on the matrix system and chosen cure cycle. As the cross-linking of the thermoset continues, the  $T_g$  increases. Curing above the  $T_g$  facilitates segmental motion of the polymeric chains in the matrix, allowing easier curing. However, when the  $T_g$  approaches the curing temperature, the matrix transitions from amorphous to glassy state. Consequently, the segmental motion of the polymeric chains drastically reduces and thereby slows down the curing process. This event is called the point of vitrification.

A consequence with thermosetting matrices as the degree of cure increases is the cure-induced volumetric shrinkage caused by the crosslinking. The cure-induced volumetric shrinkage is unique for every system, but a typical cure-induced volumetric shrinkage of an epoxy is 3.5 – 4.5 % [16,17]. To end the cure cycle, the temperature is lowered to room temperature with a ramp-down. The decrease in temperature causes further shrinkage of the cured component due to thermal contraction. These two combined, the cure-induced volumetric shrinkage of the matrix, and the different thermal expansions of the fibres and thermoset matrix during the cool down builds up residual stresses in the cured component. This happens no matter the shape of the component, from flat to formed laminates. The more complex the part, such as a T-profile (see Fig. 6), the residual stresses become more complex, affecting their mechanical properties after cure. Today, the development of composite manufacturing is towards more complex and co-cured composite components to cut costs and to save weight. The weight saving is primarily due to the reduction in the number of fasteners required and consequently the redesign of the laminate, not requiring dimensioning of the design of the laminate's thickness for bearing stress. Therefore, these increasingly complex structures will require monitoring, equally during manufacturing/curing, and later during their operational life. Today, cure monitoring of aerospace composite parts is rudimentary, monitoring the laminate temperature with thermocouples in the edges and monitoring the vacuum in the tube to the vacuum bag. In the future, ideally, it would be of interest to measure and/or monitor the following during the curing and processing of thermosetting polymers:

- $T_g$  of uncured prepreg
- Viscous flows of matrix during consolidation
- Degree of cure
- Viscosity of matrix
- The gel point
- The point of vitrification
- Residual stresses

The potential to better monitor the cure cycle is attractive and has been investigated in paper B “*In-situ cure monitoring of structural composite by embedment of vertically aligned carbon nanotube forests.*” in this thesis.

## 3 Nanomaterials for Embedded Sensing

An approach to achieve embedded sensing in FRPCs is with the use of nanomaterials. Here, their use may range from the choice of nanomaterial, the properties of the chosen nanomaterial, the morphology of the sensing structure, and the choice of measurement method. Properties of interest for the chosen nanomaterials can be conductive, semiconductive, dielectric, and more. From the properties that the nanomaterial possesses, the morphology and aim of the sensing structure should be defined. What should be measured by the sensor? Where should the sensing be performed? What production method is used to manufacture the FRPC? These questions are good to have in mind when designing and planning for the sensing.

In literature, the most studied nanomaterials for sensing applications in connection to FRPCs or polymer composites are carbon black [18–21], carbon nanotubes (CNTs) [9,10,22–46], and graphene [27,47–57], with some emerging materials as MXenes [58–61] gathering interest. However, in this work, the carbon-based nanomaterials CNTs and graphene are in focus, with an emphasis on CNTs.

### 3.1 Graphene and Carbon Nanotubes

The discovery of graphene and CNTs have both contributed to the field of nanomaterials. Graphene is a single layer of carbon atoms arranged in a hexagonal structure and bonded together by  $sp^2$  carbon-carbon orbitals. Due to its structure, pure graphene is a zero-band gap semiconductor on the border between metallic and semiconducting behaviour [62]. Due to its exceptionally

high charge carrier mobility [63] and the remaining unhybridized p-orbitals extending out-of-plane to form a delocalized pi-bonding system, graphene possesses high electrical conductivity [64].

CNTs share the hexagonal carbon-carbon structure with graphene. However, instead of a 2-dimensional structure, the hexagonal structure is rolled up, forming a nanotube. The electrical properties of CNTs have proved to be complex. The chirality, describing the hexagonal structure of the tube along its axis, i.e. how the graphene closes to become a tube, is described by a vector, the chiral vector:

$$C_h = na_1 + ma_2 \quad (1)$$

where  $a_1$  and  $a_2$  are the unit vectors in the hexagonal lattice,  $n$  and  $m$  are integers indicating the length and direction of the chiral vector based on the unit vectors, see Fig. 8 for examples. From the chiral vector, it is also possible to calculate the diameter of a single-walled CNT (SWCNT):

$$d = \frac{a}{\pi} \sqrt{n^2 + nm + m^2} \quad (2)$$

the unit vector  $a$  being 0.246 nm [65]. In addition, it has been discovered that if  $(2n + m)$  equals a multiple of 3, the SWCNT's electronic structure is metallic. From this, it is determined that  $1/3$  of all SWCNTs are metallic and  $2/3$  are semiconducting, see Fig. 8 for more examples.



Figure 8: Chirality of carbon nanotubes. Integers inside the hexagons are  $n$  and  $m$ , describing the chiral vector

Additionally, the electronic band gap of semiconducting SWCNTs is dependent on the tube diameter, becoming smaller as the diameter increases [66,67]. Excellent current capacity has been observed in individual CNTs, exceeding those of highly conductive metals. It has been determined that the impressive current capacity of individual CNTs is due to ballistic conduction [68], being reported in both metallic [69–71] and semiconducting [72,73] SWCNTs as well as in multi-walled CNTs (MWCNTs) [74–77]. However, diffusive conduction has also been observed in experiments using MWCNTs [69,78]. By definition, ballistic conduction in CNTs occurs when the electron mean free path is longer than the conduction channel, i.e., the length of the CNT. The electron mean free path of CNTs depends on their structure, increasing with an increase in diameter [71], and decreasing with an increase in the number of dislocations and impurities, acting as scattering sites [79]. MWCNTs, which are commonly described as consisting of several concentric SWCNTs, have an electronic behaviour depending on their constituent tubes. However, it has been concluded that most individual MWCNTs exhibit metallic properties [62,80].

At this time, it is difficult to control all these parameters of CNTs during production, especially the chirality of SWCNTs, which has held back the progress of using CNTs in microelectronics. For applications relevant to this work, with embedded sensing in FRPCs, the properties of individual CNTs and/or graphene are not the target. Rather, larger conductive structures consisting of CNTs or graphene are of interest.

### **3.2 Conductive Structures and Percolated Systems**

Several sensing structures out of graphene and CNTs have been reported in literature. Using graphene, coatings on fibres [27,47,48], papers and films [49–57], and nanocomposites, i.e., nanomaterial dispersed in a polymer matrix [81,82] have been reported to measure strain [49–54,56,57,81,82], temperature [55,81], and to monitor the curing and processing of thermosetting polymers [27,47,48].

Similarly, sensing structures consisting of CNTs have been reported in literature in the form of coatings on fibres [22–28], sheets and buckypapers (paper morphology using CNTs) [29–35], yarns [43], nanocomposites [25,36–42], and forests [9,10,44–46]. The CNT structures have been used to measure strain [9,23,25,31–33,37–41,44], temperature [9,29,30,33,36,42,45,46], pressure [22,43,44], and to monitor the curing and processing of thermosetting polymers

[10,23,24,26–28,30,34,35]. In the mentioned works above, the dominant measurement method for sensing is the measurement of resistance under direct current conditions.

Fundamental work done by Skákalová et al reported in [83] studied conductive networks only consisting of SWCNTs. Four “thin networks” are studied and a buckypaper of SWCNT, where the thin networks are added in SWCNT deposition from one to the next, network 1 being the thinnest (network 4 = 4 x network 1). Here, the thinnest conductive SWCNT network reveals a semiconductive behaviour in I-V sweeps, especially pronounced at low temperatures, whilst the thicker networks show more ohmic behaviour. Later, measuring the temperature dependence of the conductance of the networks, the thinnest network’s conductance goes towards zero as the temperature approaches 0 Kelvin (4.3 Kelvin). The thicker networks also decrease their conductance as the temperature drops, however, the conductance remains higher as the temperature approaches 0 Kelvin. In contrast, the SWCNT buckypaper retains 40 % of its room temperature conductivity when approaching 0 Kelvin, exhibiting metallic behaviour. This work indicates the influence of the nanomaterial chosen in the conductive network. The semiconductive response of the thinnest network is caused by the intrinsic properties of the SWCNTs, where 2/3 are semiconductive due to their chirality and 1/3 metallic (see Fig. 8). The conductive networks span a distance by propagating charge carriers, i.e. electrons, from one SWCNT to another in the networks. The number of conduction paths depends on the concentration of SWCNTs (in this work) and the current flows through the channels of least resistance, i.e. principle of least resistance. Due to this, if the network is sufficiently sparse, SWCNTs with semiconducting properties will define the conduction path of the current, hence why semiconducting behaviour is observed. As the network gets thicker, more conduction channels appear and the chance of them being dominated by metallic SWCNTs increases, transitioning towards the ohmic behaviour, ending up in a saturated SWCNT network in the SWCNT buckypaper. Although this study is not necessarily applicable to sensors in FRPCs, it explains the fundamentals of the conductive networks using SWCNTs and the importance of knowing which nanomaterial is used, as the choice of nanomaterial may influence the conductive network.

In practice, most of the reported sensing structures mentioned above use MWCNTs. As previously stated, most MWCNTs possess metallic properties, and the conductive networks of these are described by statistics and the number of

conduction channels. This is described by percolation theory. As the sensing structures are going to be embedded within FRPCs, they will by their embedment be infused with polymer resin. Percolation in polymer composites describes the transition from an electrically insulating material to a conductive one as conductive fillers are added and begin to form a continuous network of conductive particles. At low filler contents, conductive particles are isolated within the polymer matrix and electrical transport is negligible because charge carriers cannot move between fillers. As the filler concentration increases, particles approach one another and the probability of forming conductive pathways rises. Once a critical concentration, known as the percolation threshold, is reached, a continuous or quasi-continuous network spans the material, enabling long-range charge transport. Beyond this point, the composite's DC conductivity increases sharply, often by several orders of magnitude, with further filler addition. The nature of the percolating network depends strongly on the filler morphology. Carbon black consists of roughly spherical or fractal aggregates with relatively low aspect ratios. As a result, a relatively high-volume fraction is required before particles touch or come close enough to form a continuous network. CNTs, by contrast, are one-dimensional fillers with extremely high aspect ratios. Their elongated geometry allows them to span large distances in the polymer matrix, dramatically reducing the percolation threshold compared with carbon black. A conductive network can form with very low percolation thresholds, sometimes below 0.1 wt% [84], depending on the form factor of the CNTs and matrix. This is illustrated in Fig. 9.

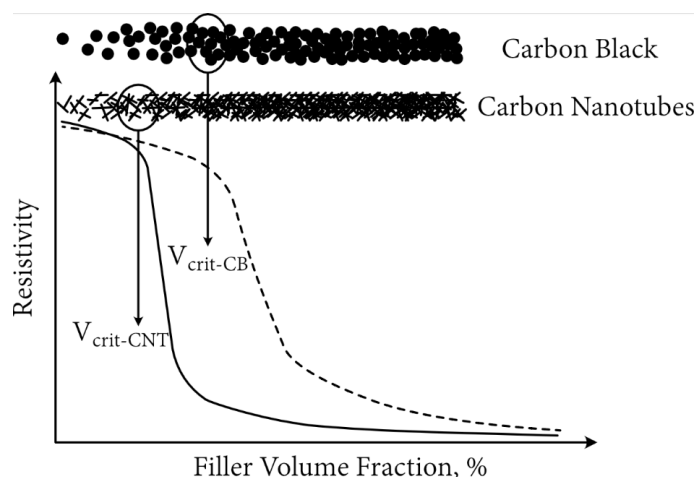


Figure 9: Illustration of CNT network percolation threshold, compared with carbon black

Graphene-based composites occupy an intermediate regime. Graphene and graphene nanoplatelets are two-dimensional fillers with high in-plane conductivity and large surface areas but lower effective aspect ratios than CNTs when dispersed as platelets. Their percolation thresholds are typically lower than those of carbon black but higher than those of CNTs, depending on flake size, thickness, and dispersion quality.

### 3.3 Sensing Mechanisms

The majority of work using conductive CNTs (and graphene) structures for sensing applications has used DC in order to measure their resistive response to stimuli. An easy representation of the resistance of a CNT conductive structure can be given by Eq. 3:

$$R_{Total} = R_{CNTs} + R_{Junction} + R_{Tunneling} \quad (3)$$

, where the total resistance of the sensor and conductive structure is dependent on three factors, being the: i)  $R_{CNTs}$ , the intrinsic resistance of the CNTs in the conductive network. ii)  $R_{Junction}$ , the resistance of the junctions between CNTs, consisting of the physical contact resistance between CNTs, and iii)  $R_{Tunneling}$  the tunnelling resistance between CNTs. This equation will serve as a base when discussing the resistive response of CNT-based sensors (and graphene) embedded in polymer during their production and later during their operational life.

#### 3.3.1 Production and Cure Monitoring

As mentioned previously, CNT and graphene conductive structures have been used for process and cure monitoring of FRPCs. CNT conductive structures in the form of coatings on fibres have been used to monitor the processing and curing using VARTM [26–28]. In these works, the flow front of the matrix [26] and the resin infiltration into the CNT structure [27] has been monitored. Similarly, buckypapers [30,35] and SWCNT coated fibres [23] have monitored the resin infiltration of the conductive structures in prepreg systems. These occurrences appear as a significant resistance increase. The resistance increase observed is due to changes in the  $R_{Junction}$ , where the infiltration of resin into the conductive network breaks up CNT-CNT contacts (physical). Simultaneously, the resin infiltration introduces a polymer into the CNT-CNT

junction, increasing the potential barrier for the tunnelling to occur at the same time also increasing the inter-distance between CNTs, increasing  $R_{Tunneling}$ . Collectively, these are conclusions in the literature given to the increase of resistance in CNT and graphene structures as resin is infiltrating the structures. The resin infiltration is noticed as a resistance peak in these works, followed by a resistance decrease. In [27], the peak was correlated to the gel-point in the VARTM process, using a polyester resin. The subsequent resistance decrease was determined to be due to the cure-induced volumetric shrinkage. It is known from literature that the significant shrinkage occurs after the gel-point [16,17]. The cure-induced volumetric shrinkage of the polyester affects the  $R_{Tunneling}$ , decreasing the distance between individual CNTs, therefore decreasing the tunnelling resistance. In the same work, the same observations and conclusions were drawn using a reduced graphene oxide (rGO) coated fabric. Other works have made similar observations and concluded that the cure-induced shrinkage is monitored using CNTs [23,35,48] and graphene [27,48].

In a paper [30], the authors attempt to determine the curing degree of their component through the temperature resistance coefficient (TCR) of embedded buckypapers, calculated from the ramp-down after having cured laminates at different temperatures. According to the authors, the TCRs from the different cure cycles can help map out and later be used to determine the curing degree. This, they claim, is caused by the shifting  $R_{Junction}$  and  $R_{Tunneling}$  of the buckypaper correlating to the different cure cycles and subsequent curing degree.

Reports in literature on the measurement of residual stresses using CNTs or graphene are few. In two papers by the same group [27,48], the authors claim to have measured a build-up of stresses onto their rGO-coated fibres caused by the cure-induced volumetric shrinkage by the matrix which is observed as a resistance increase in the post-cure. However, methods to verify the resistance increase to be caused by build-up of residual stresses needs to be presented. The same observation is not seen in the CNT-coated fibres in the same articles.

### 3.3.2 Structural Health Monitoring

#### 3.3.2.1 Deformation

The use of CNT and graphene conductive structures to perform SHM has been exemplified above, measuring strain, pressure and temperature. Regarding strain and pressure, the sensor's signal originates from a deformation of the conductive network. Discussing Eq. 3 again, the mechanisms of the piezoresistive effect in CNT/polymer-based sensors are:

- i) the piezoresistive effect from individual CNTs [33,37]
- ii) the break-up of conductive paths in the percolated system [25,85,86]
- iii) change in tunnelling distance between CNTs [37–39]

Which effect is dominant depends on the CNT architecture, the aspect ratio of the CNTs, and the studied strain range. A common strategy to achieve higher sensitivity of the sensor is to design the sensor's CNT (or graphene) content to be close to the percolation threshold. Since the percolation threshold consists of a major resistivity change in a narrow concentration interval, small changes in inter-particle distance are envisioned to produce highly sensitive sensors. The drawback of this method is dispersion and agglomeration issues with CNTs and graphene due to their high surface area facilitating agglomeration. The other strategy is to avoid the percolation threshold, using a saturated conductive network. Under these conditions inter-particle distance is not as significant an effect. Rather, saturated systems tend to have lower sensitivity and often their piezoresistive response caused by the collective piezoresistive response of the individual nanomaterial, i.e. changing the  $R_{CNTs}$ , see Eq. 3.

More than one of the piezoresistive mechanisms mentioned above can be present in a sensor using CNTs, depending on which strain interval is studied. Boztepe et al. [31] embedded a buckypaper layer into a carbon-fibre/epoxy composite, electrically insulating the buckypaper from the surrounding conductive carbon fibre by introducing an epoxy adhesive film. This ensured that the electrical conduction occurred solely through the buckypaper. During fatigue testing, the sensor exhibited an initial negative parabolic piezoresistive response up to 0.4% strain. This behaviour was attributed to the Poisson-induced transverse compression of the buckypaper, which reduced the tunnelling distance between adjacent CNTs. Beyond this strain level, the response transitioned into a positive and linear piezoresistive behaviour. Similarly, Aly et al. [32] investigated embedded aligned buckypapers in

glass-fibre/epoxy composites for damage detection and strain monitoring. The sensor exhibited a negative linear piezoresistive response up to 0.6% strain, also attributed to the Poisson effect, reducing the inter-tube distance within the CNT-network. Beyond this point, the response shifted to a positive and linear piezoresistivity until failure. The transition in behaviour was attributed to the intrinsic piezoresistivity of individual CNTs, progressive damage accumulation within the composite, and a reduction in contact points between the stacked buckypaper layers. Luo et al. [23] investigated SWCNT-coated fibres for lifelong sensing in FRPCs. Using a spray-coating technique, SWCNTs were deposited onto the surfaces of glass, polyaramid, and nylon fibres, which were subsequently embedded within the interlaminar region of glass-fibre/epoxy prepreg laminates. The sensors exhibited distinct piezoresistive behaviours depending on their orientation relative to the applied load. When aligned with the loading direction, the transverse compressive strain induced by the Poisson effect caused a reduction in inter-tube distance within the resin-infiltrated CNT coating, resulting in a negative piezoresistive response. Conversely, when positioned perpendicular to the applied load, tensile strain in the fibre's transverse direction increased the inter-tube spacing, producing a positive piezoresistive response. Lastly, Yin et al. [37] reported that the piezoresistive response of their CNT-based nanocomposites was governed by the collective piezoresistive behaviour of the individual nanotubes. They concluded that the aspect ratio of the CNTs dictates the dominant sensing mechanism: nanocomposites incorporating CNTs with lower aspect ratios ( $>100$ ) exhibited tunnelling-dominated piezoresistivity, whereas those containing higher-aspect-ratio CNTs (500–1500) demonstrated piezoresistivity driven primarily by the intrinsic piezoresistive properties of the nanotubes themselves.

### **3.3.2.2 Temperature**

Typical metallic behaviour is characterised by an increase in resistance with increasing temperature, arising from phonon-scattering events. This behaviour has been observed in both individual metallic SWCNTs [87] and in dense SWCNT networks [83]. In contrast, the negative resistance–temperature coefficient (NRC) behaviour reported for most CNT-based temperature sensors is commonly attributed to either variable-range hopping (VRH) or fluctuation-assisted tunnelling (FAT) mechanisms [80]. VRH, frequently observed in semiconducting materials, involves charge transport via thermally activated hopping between localised states. FAT, on the other hand, describes conduction

through metallic channels embedded within an insulating matrix, where tunnelling between adjacent metallic regions is facilitated by thermal fluctuations. The dominant transport mechanism in a given CNT architecture depends on the CNT volume fraction within the percolated network, as well as on whether SWCNTs or MWCNTs are used [62,83].

### **3.3.3 Direct Current versus Alternating Current for Sensing**

In the literature, resistance measurements under DC conditions are the dominant approach when using CNT- or graphene-based conductive structures for sensing in FRPCs. In contrast, only limited work has explored sensing using AC methods. This thesis examines this gap further in Paper E, where AC measurements are investigated, exploring dielectric behaviour, sensing capabilities, and frequency-dependent effects.

## 4 The VACNT Forests and Embedment into FRPCs

In this work, the VACNT forests from N12 Technologies have been used to evaluate their sensor properties when embedded into structural composites. Grown on a stainless-steel substrate through a chemical vapour deposition (CVD) method, the VACNT forests were still attached to the substrate upon delivery and used without further modification. Previously studied as z-reinforcement, the VACNT forests are known to not deteriorate the mechanical properties of the laminates [88–91], which further justifies their suitability as embedded sensors. In this work, the laminates have been produced using preregs. In order to embed the VACNT forests into the lay-up prior to curing, the VACNT forests have been deposited onto prepreg surfaces. This can be seen in Fig. 10 below, where in Fig. 10 a, where a substrate with the as-grown VACNT forests (black) rests on top of a glass fibre prepreg. Later, in Fig. 10 b, is the same glass fibre prepreg with VACNT forests deposited onto the surface.

The deposition was performed in a set-up consisting of a heating plate, encapsulated by a vacuum bag connected to a vacuum pump. Using this set-up, both temperature and vacuum can be controlled. To deposit the VACNT forest, the prepreg was placed on top of the heating plate followed by the stainless-steel substrate on top of the prepreg, with the VACNT forest facing the prepreg surface. Thereafter, the vacuum bag was sealed. The heating plate raises the temperature of the prepreg, monitored by thermocouples, to a predetermined temperature (depending on which prepreg system is used). As the prepreg reaches the predetermined temperature, the vacuum is applied, and the vacuum

bag presses down the substrate onto the surface. After some time, which depends on the prepreg system used, the vacuum is released, the vacuum bag opened and the stainless-steel substrates removed, leaving behind the VACNT forests on the prepreg surface.

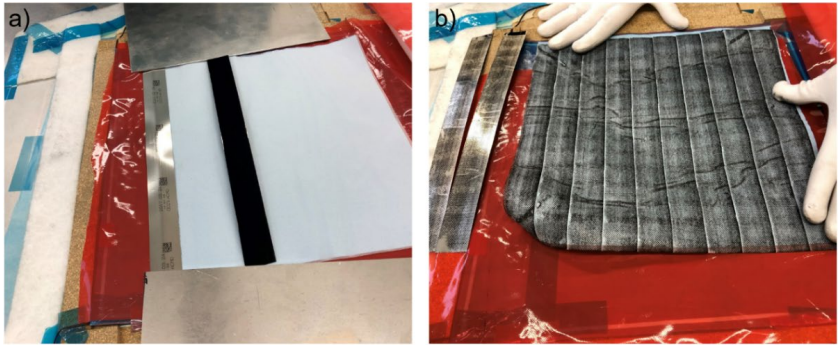


Figure 10: a) Glass fibre prepreg with VACNT forests on stainless steel resting on top. b) Glass fibre prepreg with VACNT forest deposited onto prepreg surface. Reprinted from paper A [9] without changes

With this simple deposition method, it is possible to place the sensor anywhere during the lay-up of the laminate for localised sensing. After the deposition, moving to the lay-up of the laminate, the deposited VACNT forests need to be contacted with a material functioning as an electrode in order to perform resistive measurements on the embedded VACNT forests. The selected material to function as electrodes has been a variety of carbon fibre veils of different surface weights and with/without different metal coatings, provided by Technical Fibre Products Ltd, now James Cropper PLC. Measurements on the embedded VACNT forest have only been performed in one interlaminar region per sample, building thickness around the interlaminar region. An illustration of a standard sample is presented in Fig. 11. Most work in this thesis has been performed on a coupon level.

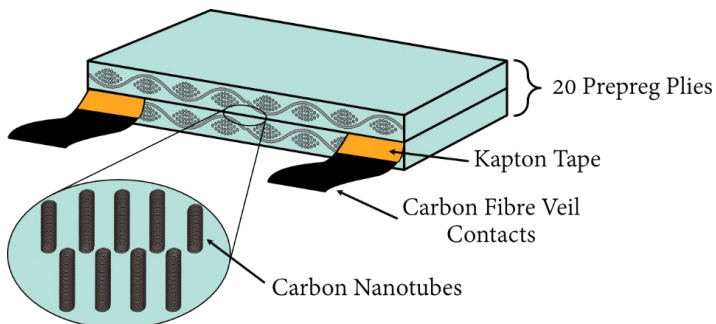


Figure 11: Sample used in papers A, B and D

During and after curing, the contacts are connected to the measurement device, performing the measurements presented in this work.

Prior to studying the sensing functionalities of the embedded VACNT forests, a characterisation of the as-received VACNT forests was performed. Individual CNTs were studied using Transmission Electron Microscopy (TEM), see Fig. 12 and the VACNT forest was studied by Scanning Electron Microscopy (SEM) when still attached to the substrate. This was motivated by requiring a fundamental understanding of the nanomaterial used in this research, the number of walls of the CNTs, and the height of the forest, in order to eventually determine the volume fraction of CNTs embedded into the CNT-rich region of the laminates. Through this process, it was decided that the conductive network was saturated, not close to the percolation threshold. More information is found in paper A.

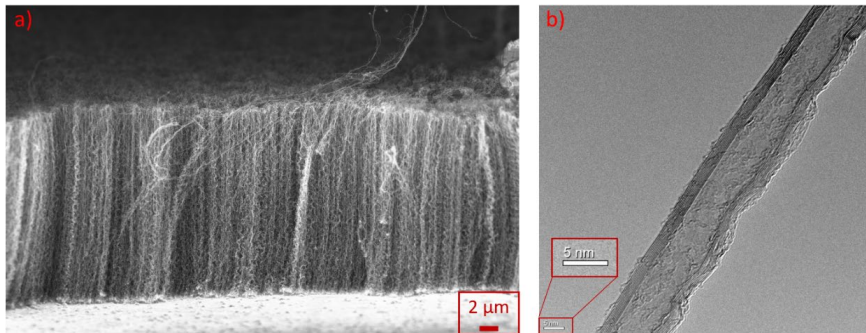


Figure 12: a) SEM of the VACNT forest still attached to the stainless-steel substrate. Credit to Thirza Poot at Linköping University. b) TEM picture of an individual CNT from the VACNT forest. Credit to Fang Liu at Chalmers University of Technology. Reprinted from Paper A [9] without changes



## 5 Comparison with Optical Methods for Embedded Sensing

Fibre optical sensing methods are typically classified into three categories based on their working principle: Grating-based sensors, interferometric sensors and distributed sensors [92]. Out of these, fibre Bragg grating (FBG) sensors are by far the most used for embedded sensing within FRPCs. FBGs have been used in a pre-study for benchmarking CNT-based sensing during this thesis. A FBG is fabricated by illuminating a short section of the core of a single-mode fibre with a periodic pattern of laser light. This process creates a permanent refractive index modulation according to the exposure pattern, called a grating. As light travels through this region in the FBG, a small amount of light is reflected at each periodic refraction change. When the wavelength of the light source is twice the grating period, the reflected components interfere constructively, producing an intense reflected signal. The wavelength at which this reflection occurs is called the Bragg wavelength [93]:

$$\lambda_{Bragg} = 2n\Lambda \quad (4)$$

where Bragg wavelength,  $\lambda_{Bragg}$ , depends on the index of refraction,  $n$ , and the spatial period of the grating,  $\Lambda$ . Therefore, any external phenomena or stimuli that affect either of the two parameters will create a shift in the Bragg wavelength. Since both parameters have linear strain and temperature dependence, so will the Bragg wavelength. Fig. 13 illustrates the application of FBGs as strain sensors.

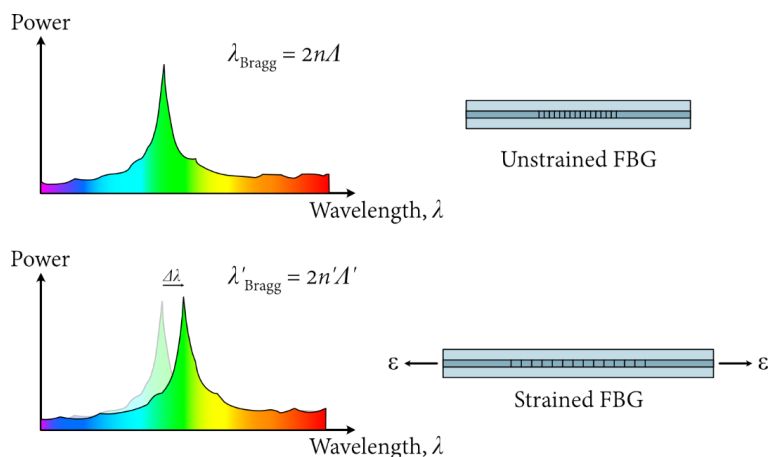


Figure 13: Working principle of an FBG

FBGs have been widely employed for SHM due to their capability to be seamlessly embedded into materials, immunity to electromagnetic interference, high multipoint sensing capability in a single optical fibre and high sensitivity to strain and temperature [92].

FBGs have been embedded into FRPCs to measure strain [94,95], temperature [95,96], and to monitor the processing and cure of thermosetting polymers [96–98]. However, although the FBG and its system are a mature sensing technique, several practical challenges remain for the reliable use of FBGs as embedded sensors in FRPCs:

- Interaction with the surrounding composite:**  
The adhesion between the optical fibre and the FRPC governs how stresses are transferred to the FBG. Variations at this interface influence the accuracy and interpretation of the measured signal.
- Temperature-related constraints:**  
Differences in the coefficient of thermal expansion (CTE) between the fibre and the composite can introduce additional strain components. Whether the fibre is free to expand thermally or constrained by the laminate should be considered.
- Complex signal interpretation:**  
Because the FBG responds to strain in the fibre itself, interpreting the signal becomes challenging in environments where both temperature and mechanical loads vary simultaneously.

- **Handling and manufacturing limitations:**  
FBGs are fragile and difficult to embed without damage. Where the fibre exits the laminate, it is particularly susceptible to bending during vacuum bagging, which can permanently degrade or extinguish the signal.
- **Limited capability during processing:**  
Since the sensor responds to deformation of the optical fibre, it is not suitable for detecting resin flow or similar phenomena during manufacturing.

### 5.1 Pre-study Benchmarking using FBGs

Presented in this section are results from trials using embedded FBGs in glass fibre laminates, monitoring the bending of the laminate. The measurements were performed at an early stage of the thesis as a pre-study benchmarking using a mature sensing technique for embedded sensing, to which later resistive CNT-based measurements could have early comparisons. The FBG-based measurements were performed by the Fiber Optics and Photonics Unit at RISE, Research Institute of Sweden.

Samples with FBGs and VACNTs were manufactured in parallel. The samples were produced of 20 glass fibre prepreg plies in thickness, placing the sensors 5 plies into the laminate from one surface. Due to bending being studied in the pre-study, it was essential to place the FBG or VACNT forest offset from the neutral midplane to experience bending-induced compression or tension, depending on which side of the sample laminate the bending was performed. Due to this, the samples were tested from both sides in an effort to measure the effects of tension and compression.

Three-point bending was performed, using a 120 mm distance between the supports. The tests were performed in an Instron 4505. For the FBG samples, the mid-point of the sample was vertically displaced 5 mm, bending the sample. The measured and converted micro-strain by the FBG is presented in Fig. 14. For the VACNT sample, the same set-up was used, however, the vertical displacement was increased to 10 mm. The resistance response of the embedded VACNT forest to the bending is presented in Fig. 15.

Observing Fig. 14, the measured micro-strain of the embedded FBG is presented; a) in tension configuration and b) in compression configuration. The FBG is able to detect strain in both tension and compression and is a sensitive measurement with a linear response to the vertical displacement.

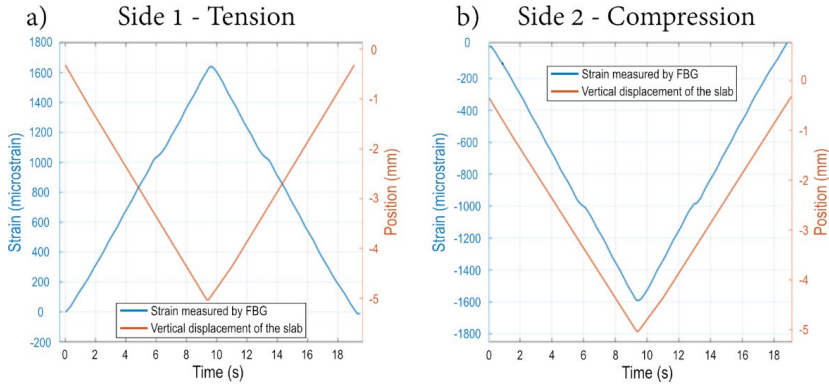


Figure 14: Bending measured by the FBG in (a) tension configuration and (b) compression configuration

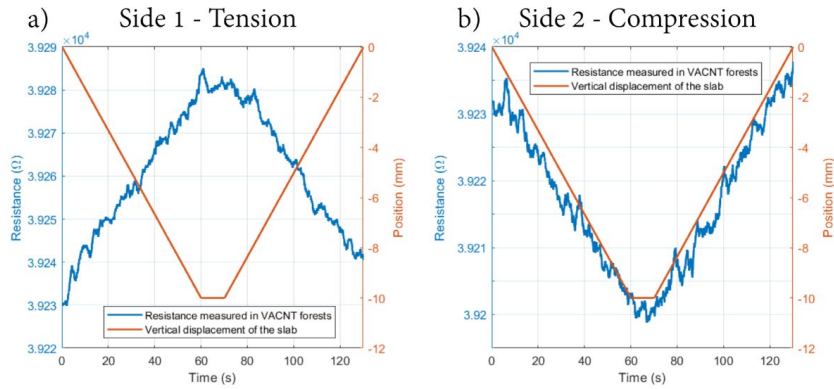


Figure 15: Bending measured by VACNT in (a) tension configuration and (b) compression configuration

Similarly, the resistive measurements on the embedded VACNT forests have captured bending caused by tension in Fig. 15 a. This is further strengthened in paper A, where a resistance increase is measured in embedded VACNT forests during tensile testing. Bending the sample from the other side, Fig. 15 b, the embedded VACNT forest is in the region experiencing compression. The resistance decrease indicates that the embedded VACNT forests are susceptible to compression. Although the resistive measurements are suffering from noise, they also exhibit a linear trend in response to the vertical displacement. In addition, the sensitivity of the resistive measurements is low. However, the comparison between the mature and established FBG-based sensing system and the resistive measurements on the VACNT forest was valuable early in the work leading up to this thesis. The results encouraged the continued work and refinement of the measurement method using VACNT forests instead of continuing to other conductive structures.

## 6 Summary of Papers

The appended papers collectively address the thesis aim of developing and evaluating embedded nanomaterial-based sensing concepts, primarily VACNT forests, for both manufacturing monitoring and structural health monitoring of composite materials. The work progresses from fundamental characterisation of the VACNT forests to their integration into prepreg laminates, followed by resistive *in-situ* cure monitoring of thermosetting prepreg laminates, strategies for sensing in conductive carbon fibre environments, comparisons with alternative nanomaterials such as graphene, and finally the introduction of AC-based impedance measurements to expand sensing capabilities. This chapter summarises how each paper contributes to these themes and clarifies the specific role each plays in advancing embedded sensing in fibre-reinforced polymer composites.

**Paper A** – *Sensing abilities of embedded vertically aligned carbon nanotube forests in structural composites: From nanoscale properties to mesoscale functionalities.*

The paper presents a thorough characterisation of VACNT forests and their use as resistive sensors when embedded into two different glass fibre/epoxy systems. A bottom-up approach has been adopted, starting with an initial study of the used VACNT forests prior to being deposited onto prepreg surfaces and subsequently embedded into the laminate. This involved a TEM study of individual CNTs from the VACNT forests, determining their thickness, number of walls and the spread of these. Thereafter, a SEM study of the VACNT forest was conducted, determining the height of the forest. The weight of the VACNT forests was determined by Thermogravimetric Analysis (TGA). The results from the TEM and SEM helped determine the aspect ratio of CNTs, and the weight from the TGA helped determine the volume fraction of the CNTs in the VACNT forest, important data to better understand the percolation network of the VACNT forest once deposited into the laminates, where it was evaluated as a strain and temperature sensor. The characterisation determined the percolated CNT network to be saturated, not being close to the percolation threshold, influencing the sensing mechanism. The ohmic nature of the sensor is determined by the linearity seen in voltage-current sweeps, expected from a percolated network of multi-walled CNTs. These observations are/were input required for the determination of the sensing mechanisms to temperature and strain. First, the thermoresistive behaviour was determined to be caused by Fluctuation-Assisted Tunnelling, reported for between metallic particles (The MWCNTs) in a non-conductive environment (the epoxy). Secondly, the linear piezoresistive response to strain is determined to be caused by the collective piezoresistive effect of individual CNTs in the sensor, as the system is determined to be saturated and therefore not sensitive to changes inter-distance between CNTs at the studied strain interval (up to 1 % strain). These conclusions were based on the bottom-up approach used, explained from nanoscale properties up to mesoscale functionalities.

**Paper B** – *In-situ cure monitoring of structural composite by embedment of vertically aligned carbon nanotube forests.*

The paper investigates *in-situ* resistive cure monitoring of aerospace-grade glass fibre/epoxy prepreg laminates performed by embedded VACNT forests. The measured resistance during the cure cycle is interpreted by studying the morphology of the VACNT forest, cure kinetics and viscosity of the resin, and volumetric changes of both resin and laminate during sections of the same cure cycle. From these studies, the resistive signal is determined to detect the transition between the air-evacuation and consolidation regimes of the laminate compaction and the gel point of the epoxy. Interestingly, the measurements do not appear to be directly sensitive to the cure-induced shrinkage in this epoxy system. Rather, a resistance increase is observed after the gel-point, where a resistance decrease would be expected from a cure-induced shrinkage. The increase in resistance is theorised, therefore, to be caused by the build-up of residual stresses in the glass fibre/epoxy laminate, appearing due to the interplay between the cure-induced shrinkage of the epoxy and the fixed fibre bed of the laminate. This is further supported by the fact that the mentioned resistance increase is not observed when curing an epoxy film according to the same method, without the glass fibres. The proposed cure monitoring sensor system offers great flexibility, being able to monitor the curing process locally anywhere in the laminate. Additionally, the proposed sensor offers a lifelong multifunctionality to the produced component, possessing strain and temperature sensing capabilities in the cured state, ideal for SHM, already established in paper A.

**Paper C** – *Isolation strategies of carbon nanotubes for resistive sensing in carbon fibre prepreg laminates.*

Paper C approaches the challenge of performing resistive sensing in a conductive carbon fibre environment. The study looks into two strategies to isolate the resistive sensor, VACNT forests, from the carbon fibre by adding a barrier between the two. The first strategy involves a non-permeable separator, a Kapton film, placed between the VACNT forest and the carbon fibre structure, avoiding physical contact. However, the method requires the addition of an epoxy film in order to deposit the VACNT forest and build thickness in the sensing region. The second strategy involves the use of a permeable separator. This approach utilises a consolidation step prior to curing, where the permeable separator is infused by resin from the prepreg stack, leaving an epoxy layer on its surface onto which the VACNT sensor can be deposited, separating it from the carbon fibres. The two strategies are monitored during the curing of laminates to ensure the integrity of the sensors remains intact. Thereafter, the sensors are tested in the cured components as temperature and strain sensors.

**Paper D** – *Comparative study of graphene coated glass fibers and carbon nanotube forests as embedded structural health monitoring systems.*

Paper D evaluates a graphene coating on glass fibre weave as an embedded sensing material in glass fibre/epoxy composite. Due to no prior experience working with graphene, the new material was compared to previous work on VACNT forests as sensors as a baseline. Initially, the graphene coating is evaluated as a resistive cure-monitoring sensor when embedded in a thermosetting glass fibre/epoxy laminate during manufacturing. The graphene coating exhibits a resistive behaviour comparable to that of the VACNT forests during curing. However, unlike the VACNT sensors, the graphene coating shows a distinct divergence in its resistive response upon reaching the cure temperature, characterised by a continuous decrease in resistance. This behaviour suggests sensitivity to cure-induced shrinkage of the epoxy, a response not observed with CNT sensors. In the cured state, the embedded graphene coating demonstrates excellent temperature-sensing capability, exhibiting a negative thermoresistive effect. In contrast, its strain-sensing performance is inferior to that of embedded CNT sensors, as it displays an initial resistance drift during the first loading cycle, additional drift under constant strain, and further drift upon unloading.

**Paper E** – *Sensing of Transverse Pressure in Structural Composite by Impedance Spectroscopy on Embedded Carbon Nanotube Sensing Structures.*

In this paper, two sensing structures using CNTs are evaluated as pressure sensors. Embedded into an aerospace-grade glass fibre/epoxy prepreg laminate, the sensing structures measure pressures up to 20 MPa. The paper explores a transition in sensing measurements based on direct current to alternating current in pursuit of higher sensing sensitivity using impedance spectroscopy. The first sensing structure is embedded VACNT forests, as these have been studied before. The second sensing structure, two embedded VACNT forests with a Kapton film separating them is emulating a capacitor structure in the thickness direction of the laminate. This sensing structure would not have been feasible using direct current. With the transition to alternating current, a characterisation of the two sensing structures is performed. The resistive and polarisation mechanisms of the two sensing structures are studied using a Faraday cage, providing a constant and stable stray capacitance while at the same time blocking outside electromagnetic interference. Thereafter, a measurement procedure is presented, evaluating the sensing structures' susceptibility to stray capacitance prior to pressure sensing.

The first sensing structure, embedded VACNT forests, exhibits sensitivity to pressure, the resistive sensitivity increasing at frequencies above the critical frequency of the system, justifying the shift from DC to AC. The reactance is also sensitive to pressure, however, around 1 MHz, insensitivity to pressure is detected, making it an interesting frequency range for sensing of other stimuli, possibly enabling multi-sensing in the same sensor, simply by the choice of measurement frequency.

The second sensing structure is two embedded VACNT forests with a Kapton film separating them. The measured impedance is determined to have a Kapton-dominated frequency range and a CNT-dominated frequency range, with a transition frequency interval in between. This is reflected in the pressure sensitivity, where the used frequency determines which constituent is measured on, the two constituents having different sensitivities to the applied pressure.



## 7 Contributions to the Field

The use of nanomaterials for embedded sensing in composite structures had not received great attention at the start of this thesis. This thesis has contributed to a greater understanding of VACNT forests as embedded sensors through the characterisation approach of the resistive measurements presented in papers A and B, and later, the potential of impedance measurements in paper E.

Paper A is, to the authors' knowledge, the first work on VACNT forests as embedded sensors in structural composites, proving to be a robust sensor system as the gauge factor does not depend on the CNT concentration, already being a saturated percolated network. Through the bottom-up approach applied in this work, studying the VACNT forest and its constituent tubes on the nanoscale, determining the CNT conductive structure to be saturated on the microscale, and up to the sensing abilities of the manufactured sample on the mesoscale, it is concluded that these piezoresistive properties are due to the intrinsic piezoresistivity of the individual tubes. A thorough bottom-up approach is essential to determine the origin of the piezoresistive response of the embedded VACNT forests to strain, an approach not often reported on in literature. Interfacial issues of the sensing structure are also avoided within the structural composite, as the VACNT forest is not a stand-alone sensor being embedded, like an FBG. Instead, the sensing system is formed whilst curing of the composite component, measuring in the matrix.

Regarding cure monitoring and paper B, a thorough characterisation of the prepreg system is performed to decipher the resistive signal. Although similar studies on other CNT structures have been presented, no work on VACNT forests has been reported. Kinetic and rheological methods have been used in

other works to interpret the resistive signal, however, paper B contributes to the cure monitoring field with its volumetric measurements on both laminates and matrix to help interpret the resistive signal. Due to this approach, it can be concluded, confidently, that cure-induced volumetric shrinkage does not affect the measured resistance directly. The use of volumetric measurements to better understand the used matrix system is recommended, as the initialisation of the cure exotherm does not signify an instant reduction in volume of the matrix, affecting tunnelling conditions. This conclusion further supports the conclusions drawn in paper A, where the changing tunnelling distance between CNTs is not dominating the measured resistance when increasing in strain, nor when decreasing with the cure-induced volumetric shrinkage. The presented work is the only reported work on cure monitoring, using CNTs, implying to be sensitive to the build-up of residual stresses during the cure cycle. In the future, the method presented in paper B is envisioned as a supporting measurement method to optimise cure cycles for thermosetting composites. With this work, together with paper A, it is demonstrated that the studied VACNT forest offers lifelong multifunctionality to the produced component, first functioning as a cure monitoring sensor and later, in the cured state, being able to function as a strain and temperature sensor for structural health monitoring.

Paper C contributes to the challenge of resistive sensing in a conductive carbon fibre structure. The work proposes two solutions to isolate the embedded VACNT sensing structure from the carbon fibre structure, avoiding short circuiting of the sensor.

Paper D presents a comparison between the use of graphene and CNTs for embedded sensing, where the interface of the studied graphene coating to the glass fibre is in focus, emphasising the importance of the embedment conditions of the sensing structure to function as a capable sensor. This involves the choice of sensing environment, i.e. in the matrix in comparison to a fibre coating, and the choice of nanomaterial, CNTs in comparison to graphene.

Paper E demonstrates the possibility to measure high transversal pressures using embedded sensing structures in structural composites. The paper justifies a transition from DC to AC-based measurements in pursuit of higher sensitivity in sensing measurements. With this transition, a characterisation and measurement procedure is presented and justified, required for reliable measurements. The higher sensitivity in the CNT configuration is based on the transition from a CNT-piezoresistive effect to a CNT-CNT junction sensitive measurement when using frequencies higher than the critical frequency. The

paper is the first reported work on embedded sensing using CNTs to measure high pressures, relevant for composite structures for fasteners. The paper contributes new ideas on embedded sensor design in structural composites, exploring a capacitor configuration for sensing applications.



## 8 Future Work

Future work, based on the appended papers in this thesis is first presented. Thereafter, thoughts and future work in the broader field are presented.

In paper A, the embedded VACNT forest is sensitive to strain and temperature. Future work needs to be carried out in how to separate the two stimuli in the signal to measure each separately. In addition, further work is required to distinguish different mechanical deformations of the sensing structure, such as bending,

In paper B, different cure cycles using the same prepreg system, HexPly 6376, should be evaluated to explore if more events can be captured with the *in-situ* resistive cure monitoring. Examples are to include an intermediate dwell during the ramp-up, other ramp-up rates and different curing temperatures. In addition, different prepreg systems should be studied with the method to conclude if the sensor is sensitive to the specific prepreg system or if the embedded CNT structure captures the same events and processes, independent of which prepreg system is used.

The resistance increase observed after the gel-point, suspected to be caused by a build-up of residual stresses, should be studied further. The cure monitoring should be applied to more complicated structures where the need for monitoring is relevant, such as in T-sections, having problems with residual stresses originating from the curing. Finally, a transition to AC for cure monitoring should be evaluated.

In paper C, the method for isolation can be improved, reducing the thickness and amount of material in the interlaminar region containing the VACNT forest.

Other avenues to avoid the VACNT forest short-circuiting to the carbon fibre structure should be explored.

In paper D, evaluating the functionalised graphene coating, the infiltration of the coating needs to be studied further. It is suspected that the initial drift in the strain sensing is caused by the coating not being infiltrated during the cure cycle by epoxy, giving a weak adhesion to the glass fibre weave. A SEM study is recommended.

In paper E, the transition from DC to AC is of interest for future work. This includes an investigation into more load cases apart from transverse pressure, e.g., strain and bending. Temperature measurements using AC measurements on the embedded VACNT forest should be investigated. Lastly, the possibility for multi-sensing using the embedded VACNT forest should be investigated, if two stimuli can simultaneously be measured in the same embedded VACNT forest, at different frequencies.

Regarding the broader field of nanomaterials, here conductive structures using CNTs or graphene, most work is performed characterising and applying the sensing structures. In the future, there should be more work on designing the sensor for the sensing purpose, not investigating the sensing capability and mechanisms of an already existing conductive structure.

## References

- [1] Zhang J, Lin G, Vaidya U, Wang H. Past, present and future prospective of global carbon fibre composite developments and applications. *Compos B Eng* 2023;250. <https://doi.org/10.1016/j.compositesb.2022.110463>.
- [2] Johannisson W, Harnden R, Zenkert D, Lindbergh G. Shape-morphing carbon fiber composite using electrochemical actuation n.d. <https://doi.org/10.17632/4zky6h8w3v.1>.
- [3] Zhang D, Yang S, Zhang S, Liu W, Pan H, Bai X, et al. Epoxy Resin/Reduced Graphene Oxide Composites with Gradient Concentration for Aviation Deicing. *ACS Applied Engineering Materials* 2023;1:1535–42. <https://doi.org/10.1021/acsaenm.3c00095>.
- [4] Niu Y, Su J, Yao J, Wang Z, Yang L, Qin Z. Construction of Energy-Efficient Electro-Thermal Anti-Icing/De-Icing System for Composite Wings Based on MWCNT Films. *Polym Compos* 2025. <https://doi.org/10.1002/pc.70556>.
- [5] Bouton K, Schneider L, Zenkert D, Lindbergh G. A structural battery with carbon fibre electrodes balancing multifunctional performance. *Compos Sci Technol* 2024;256. <https://doi.org/10.1016/j.compscitech.2024.110728>.
- [6] Johannisson W, Ihrner N, Zenkert D, Johansson M, Carlstedt D, Asp LE, et al. Multifunctional performance of a carbon fiber UD lamina electrode for structural batteries. *Compos Sci Technol* 2018;168:81–7. <https://doi.org/10.1016/j.compscitech.2018.08.044>.
- [7] Chaudhary R, Xu J, Xia Z, Asp LE. Unveiling the Multifunctional Carbon Fiber Structural Battery. *Advanced Materials* 2024;36. <https://doi.org/10.1002/adma.202409725>.

- [8] Asp LE, Bouton K, Carlstedt D, Duan S, Harnden R, Johannisson W, et al. A Structural Battery and its Multifunctional Performance. *Advanced Energy and Sustainability Research* 2021;2. <https://doi.org/10.1002/aesr.202000093>.
- [9] Karlsson T, Hallander P, Liu F, Poot T, Åkermo M. Sensing abilities of embedded vertically aligned carbon nanotube forests in structural composites: From nanoscale properties to mesoscale functionalities. *Compos B Eng* 2023;255:110587. <https://doi.org/10.1016/j.compositesb.2023.110587>.
- [10] Karlsson T, Dutta A, Hallander P, Åkermo M. In-situ cure monitoring of structural composite by embedment of vertically aligned carbon nanotube forests. *Compos B Eng* 2025;293:112105. <https://doi.org/10.1016/j.compositesb.2024.112105>.
- [11] Cender TA, Simacek P, Advani SG. Resin film impregnation in fabric prepregs with dual length scale permeability. *Composites Part A* 2013;53:118–28. <https://doi.org/10.1016/j.compositesa.2013.05.013>.
- [12] Helmus R, Kratz J, Potter K, Hubert P, Hinterhölzl R. An experimental technique to characterize interply void formation in unidirectional prepregs. *J Compos Mater* 2017;51:579–91. <https://doi.org/10.1177/0021998316650273>.
- [13] Centea T, Hubert P. Out-of-autoclave prepreg consolidation under deficient pressure conditions. *J Compos Mater* 2014;48:2033–45. <https://doi.org/10.1177/0021998313494101>.
- [14] Centea T, Grunenfelder LK, Nutt SR. A review of out-of-autoclave prepregs – Material properties , process phenomena , and manufacturing considerations. *Composites Part A* 2015;70:132–54. <https://doi.org/10.1016/j.compositesa.2014.09.029>.
- [15] Centea T, Hubert P. Measuring the impregnation of an out-of-autoclave prepreg by micro-CT. *Compos Sci Technol* 2011;71:593–9. <https://doi.org/10.1016/j.compscitech.2010.12.009>.
- [16] Khoun L, Hubert P. Cure Shrinkage Characterization of an Epoxy Resin System by Two in Situ Measurement Methods. *Polym Compos* 2010;31:1603–10. <https://doi.org/10.1002/pc>.
- [17] Shah DU, Schubel PJ. Evaluation of cure shrinkage measurement techniques for thermosetting resins. *Polym Test* 2010;29:629–39. <https://doi.org/10.1016/j.polymertesting.2010.05.001>.
- [18] Melo DS, Reis IC, Queiroz JC, Cena CR, Nahime BO, Malmonge JA, et al. Evaluation of Piezoresistive and Electrical Properties of Conductive Nanocomposite Based on Castor-Oil Polyurethane Filled with MWCNT and Carbon Black. *Materials* 2023;16. <https://doi.org/10.3390/ma16083223>.

- [19] Huang K, Ning H, Hu N, Wu X, Wang S, Weng S, et al. Synergistic effect of CB and MWCNT on the strain-induced DC and AC electrical properties of PVDF-HFP composites. *Carbon N Y* 2019;144:509–18. <https://doi.org/10.1016/j.carbon.2018.12.059>.
- [20] Zheng Y, Li Y, Li Z, Wang Y, Dai K, Zheng G, et al. The effect of filler dimensionality on the electromechanical performance of polydimethylsiloxane based conductive nanocomposites for flexible strain sensors. *Compos Sci Technol* 2017;139:64–73. <https://doi.org/10.1016/j.compscitech.2016.12.014>.
- [21] Abd Hamid FK, Hasan MN, Murty GE, Ahmad Asri MI, Saleh T, Mohamed Ali MS. Resistive strain sensors based on carbon black and multi-wall carbon nanotube composites. *Sens Actuators A Phys* 2024;366. <https://doi.org/10.1016/j.sna.2023.114960>.
- [22] Doshi SM, Thostenson ET. Thin and Flexible Carbon Nanotube-Based Pressure Sensors with Ultrawide Sensing Range. *ACS Sens* 2018;3:1276–82. <https://doi.org/10.1021/acssensors.8b00378>.
- [23] Luo S, Obitayo W, Liu T. SWCNT-thin-film-enabled fiber sensors for lifelong structural health monitoring of polymeric composites - From manufacturing to utilization to failure. *Carbon N Y* 2014;76:321–9. <https://doi.org/10.1016/j.carbon.2014.04.083>.
- [24] Luo S, Wang Y, Wang G, Wang K, Wang Z, Zhang C, et al. CNT Enabled Co-braided Smart Fabrics: A New Route for Non-invasive, Highly Sensitive & large-area Monitoring of Composites. *Sci Rep* 2017;7:44056. <https://doi.org/10.1038/srep44056>.
- [25] Gao L, Chou TW, Thostenson ET, Zhang Z. A comparative study of damage sensing in fiber composites using uniformly and non-uniformly dispersed carbon nanotubes. *Carbon N Y* 2010;48:3788–94. <https://doi.org/10.1016/j.carbon.2010.06.041>.
- [26] Dai H, Thostenson ET. Scalable and multifunctional carbon nanotube-based textile as distributed sensors for flow and cure monitoring. *Carbon N Y* 2020;164:28–41. <https://doi.org/10.1016/j.carbon.2020.02.079>.
- [27] Wang G, Wang Y, Luo Y, Luo S. Carbon nanomaterials based smart fabrics with selectable characteristics for in-line monitoring of high-performance composites. *Materials* 2018;11:1677. <https://doi.org/10.3390/ma11091677>.
- [28] Gnidakoung JRN, Roh HD, Kim J-H, Park Y-B. In situ process monitoring of hierarchical micro-/nano-composites using percolated carbon nanotube networks. *Compos Part A Appl Sci Manuf* 2016;84:281–91. <https://doi.org/10.1016/j.compositesa.2016.01.017>.

- [29] Lu S, Chen D, Wang X, Xiong X, Ma K, Zhang L, et al. Monitoring the glass transition temperature of polymeric composites with carbon nanotube buckypaper sensor. *Polym Test* 2017;57:12–6. <https://doi.org/10.1016/j.polymertesting.2016.11.008>.
- [30] Lu S, Zhao C, Zhang L, Chen D, Chen D, Wang X, et al. Real time monitoring of the curing degree and the manufacturing process of fiber reinforced composites with a carbon nanotube buckypaper sensor. *RSC Adv* 2018;8:22078–85. <https://doi.org/10.1039/c8ra03445a>.
- [31] Boztepe S, Liu H, Heider D, Thostenson ET. Novel carbon nanotube interlaminar film sensors for carbon fiber composites under uniaxial fatigue loading. *Compos Struct* 2018;189:340–8. <https://doi.org/10.1016/j.compstruct.2018.01.033>.
- [32] Aly K, Li A, Bradford PD. Strain sensing in composites using aligned carbon nanotube sheets embedded in the interlaminar region. *Compos Part A Appl Sci Manuf* 2016;90:536–48. <https://doi.org/10.1016/j.compositesa.2016.08.003>.
- [33] Li A, Bogdanovich AE, Bradford PD. Aligned carbon nanotube sheet piezoresistive strain sensors. *Smart Mater Struct* 2015;24:095004. <https://doi.org/10.1088/0964-1726/24/9/095004>.
- [34] Lu S, Chen D, Wang X, Shao J, Ma K, Zhang L, et al. Real-time cure behaviour monitoring of polymer composites using a highly flexible and sensitive CNT buckypaper sensor. *Compos Sci Technol* 2017;152:181–9. <https://doi.org/10.1016/j.compscitech.2017.09.025>.
- [35] Lu S, Chen D, Wang X, Xiong X, Ma K, Zhang L, et al. Monitoring the manufacturing process of glass fiber reinforced composites with carbon nanotube buckypaper sensor. *Polym Test* 2016;52:79–84. <https://doi.org/10.1016/j.polymertesting.2016.04.007>.
- [36] Lasater KL, Thostenson ET. In situ thermoresistive characterization of multifunctional composites of carbon nanotubes. *Polymer (Guildf)* 2012;53:5367–74. <https://doi.org/10.1016/j.polymer.2012.09.022>.
- [37] Yin G, Hu N, Karube Y, Liu Y, Li Y. A carbon nanotube / polymer strain sensor with linear and anti-symmetric piezoresistivity. *J Compos Mater* 2011;45:1315–23. <https://doi.org/10.1177/0021998310393296>.
- [38] Hu N, Karube Y, Arai M, Watanabe T, Yan C, Li Y, et al. Investigation on sensitivity of a polymer/carbon nanotube composite strain sensor. *Carbon N Y* 2010;48:680–7. <https://doi.org/10.1016/j.carbon.2009.10.012>.
- [39] Hu N, Karube Y, Yan C, Masuda Z, Fukunaga H. Tunneling effect in a polymer/carbon nanotube nanocomposite strain sensor. *Acta Mater* 2008;56:2929–36. <https://doi.org/10.1016/j.actamat.2008.02.030>.

- [40] Oliva-Avilés AI, Avilés F, Sosa V. Electrical and piezoresistive properties of multi-walled carbon nanotube / polymer composite films aligned by an electric field. *Carbon N Y* 2011;49:2989–97. <https://doi.org/10.1016/j.carbon.2011.03.017>.
- [41] Avilés F, May-Pat A, Canché-Escamilla G, Rodríguez-Uicab O, Ku-Herrera JJ, Duarte-Aranda S, et al. Influence of carbon nanotube on the piezoresistive behavior of multiwall carbon nanotube/polymer composites. *J Intell Mater Syst Struct* 2016;27:92–103. <https://doi.org/10.1177/1045389X14560367>.
- [42] Dai H, Thostenson ET, Schumacher T. Comparative study of the thermoresistive behavior of carbon nanotube-based nanocomposites and multiscale hybrid composites. *Compos B Eng* 2021;222:109068. <https://doi.org/10.1016/j.compositesb.2021.109068>.
- [43] Kim SY, Jee E, Kim JS, Kim DH. Conformable and ionic textiles using sheath-core carbon nanotube microyarns for highly sensitive and reliable pressure sensors. *RSC Adv* 2017;7:23820–6. <https://doi.org/10.1039/c7ra02215h>.
- [44] Shin UH, Jeong DW, Park SM, Kim SH, Lee HW, Kim JM. Highly stretchable conductors and piezocapacitive strain gauges based on simple contact-transfer patterning of carbon nanotube forests. *Carbon N Y* 2014;80:396–404. <https://doi.org/10.1016/j.carbon.2014.08.079>.
- [45] Koratkar N, Modi A, Lass E, Ajayan P. Temperature effects on resistance of aligned multiwalled carbon nanotube films. *J Nanosci Nanotechnol* 2004;4:744–8. <https://doi.org/10.1166/jnn.2004.109>.
- [46] Lee J, Stein IY, Devoe ME, Lewis DJ, Lachman N, Kessler SS, et al. Impact of carbon nanotube length on electron transport in aligned carbon nanotube networks. *Appl Phys Lett* 2015;106:053110. <https://doi.org/10.1063/1.4907608>.
- [47] Ali MA, Umer R, Khan KA, Samad YA, Liao K, Cantwell W. Graphene coated piezo-resistive fabrics for liquid composite molding process monitoring. *Compos Sci Technol* 2017;148:106–14. <https://doi.org/10.1016/j.compscitech.2017.05.022>.
- [48] Luo S, Wang G, Wang Y, Xu Y, Luo Y. Carbon nanomaterials enabled fiber sensors: A structure-oriented strategy for highly sensitive and versatile in situ monitoring of composite curing process. *Compos B Eng* 2019;166:645–52. <https://doi.org/10.1016/j.compositesb.2019.02.067>.
- [49] Yan C, Wang J, Kang W, Cui M, Wang X, Foo CY, et al. Highly stretchable piezoresistive graphene-nanocellulose nanopaper for strain sensors. *Advanced Materials* 2014;26:2022–7. <https://doi.org/10.1002/adma.201304742>.

- [50] Li X, Yang T, Yang Y, Zhu J, Li L, Alam FE, et al. Large-Area Ultrathin Graphene Films by Single-Step Marangoni Self-Assembly for Highly Sensitive Strain Sensing Application. *Adv Funct Mater* 2016;26:1322–9. <https://doi.org/10.1002/adfm.201504717>.
- [51] Yokaribas V, Wagner S, Schneider DS, Friebertshäuser P, Lemme MC, Fritzen CP. Strain gauges based on CVD graphene layers and exfoliated graphene nanoplatelets with enhanced reproducibility and scalability for large quantities. *Sensors (Switzerland)* 2017;17:1–17. <https://doi.org/10.3390/s17122937>.
- [52] Liu Q, Chen J, Li Y, Shi G. High-Performance Strain Sensors with Fish-Scale-Like Graphene-Sensing Layers for Full-Range Detection of Human Motions. *ACS Nano* 2016;10:7901–6. <https://doi.org/10.1021/acsnano.6b03813>.
- [53] Chun S, Choi Y, Park W. All-graphene strain sensor on soft substrate. *Carbon N Y* 2017;116:753–9. <https://doi.org/10.1016/j.carbon.2017.02.058>.
- [54] Groo LA, Nasser J, Zhang L, Steinke K, Inman D, Sodano H. Laser induced graphene in fiberglass-reinforced composites for strain and damage sensing. *Compos Sci Technol* 2020;199:108367. <https://doi.org/10.1016/j.compscitech.2020.108367>.
- [55] Liu G, Tan Q, Kou H, Zhang L, Wang J, Lv W, et al. A flexible temperature sensor based on reduced graphene oxide for robot skin used in internet of things. *Sensors (Switzerland)* 2018;18. <https://doi.org/10.3390/s18051400>.
- [56] Fu XW, Liao ZM, Zhou JX, Zhou YB, Wu HC, Zhang R, et al. Strain dependent resistance in chemical vapor deposition grown graphene. *Appl Phys Lett* 2011;99. <https://doi.org/10.1063/1.3663969>.
- [57] Hempel M, Nezich D, Kong J, Hofmann M. A novel class of strain gauges based on layered percolative films of 2D materials. *Nano Lett* 2012;12:5714–8. <https://doi.org/10.1021/nl302959a>.
- [58] Duongthipthewa A, Zhou H, Wang Q, Zhou L. Non-additive polymer matrix coated rGO/MXene inks for embedding sensors in prepreg enhancing smart FRP composites. *Compos B Eng* 2024;270. <https://doi.org/10.1016/j.compositesb.2023.111108>.
- [59] Chen X, Hui Y, Zhang J, Wang Y, Zhang J, Wang X, et al. Single multifunctional MXene-coated glass fiber for interfacial strengthening, damage self-monitoring, and self-recovery in fiber-reinforced composites. *Compos B Eng* 2023;259. <https://doi.org/10.1016/j.compositesb.2023.110713>.
- [60] Monastreyckis G, Stepura A, Soyka Y, Maltanova H, Poznyak SK, Omastová M, et al. Strain sensing coatings for large composite structures based on 2d mxene nanoparticles. *Sensors* 2021;21. <https://doi.org/10.3390/s21072378>.

- [61] Wang Y, Hui Y, Chen X, Wen K, Cheng S, Song Q, et al. Multifunctional MXene/carbon nanotubes coated glass fiber sensors for in-situ monitoring of curing process and structural health of polymeric composites. *Chemical Engineering Journal* 2024;497. <https://doi.org/10.1016/j.cej.2024.154386>.
- [62] Kaiser AB, Skákalová V. Electronic conduction in polymers, carbon nanotubes and graphene. *Chem Soc Rev* 2011;40:3786–801. <https://doi.org/10.1039/c0cs00103a>.
- [63] Morozov S V., Novoselov KS, Katsnelson MI, Schedin F, Elias DC, Jaszczak JA, et al. Giant intrinsic carrier mobilities in graphene and its bilayer. *Phys Rev Lett* 2008;100. <https://doi.org/10.1103/PhysRevLett.100.016602>.
- [64] Johns JE, Hersam MC. Atomic covalent functionalization of graphene. *Acc Chem Res* 2013;46:77–86. <https://doi.org/10.1021/ar300143e>.
- [65] Journet C, Picher M, Jourdain V. Carbon nanotube synthesis: From large-scale production to atom-by-atom growth. *Nanotechnology* 2012;23. <https://doi.org/10.1088/0957-4484/23/14/142001>.
- [66] Saito R, Fujita M, Dresselhaus G, Dresselhaus MS. Electronic structure of chiral graphene tubules. *Appl Phys Lett* 1992;60:2204–6.
- [67] Hamada N, Sawada S, Oshiyama A. New One-Dimensional Conductors: Graphitic Microtubules. *Phys Rev Lett* 1992;68:1579–81.
- [68] Wei BQ, Vajtai R, Ajayan PM. Reliability and current carrying capacity of carbon nanotubes. *Appl Phys Lett* 2001;79:1172–4. <https://doi.org/10.1063/1.1396632>.
- [69] Bachtold A, Fuhrer MS, Plyasunov S, Forero M, Anderson EH, Zettl A, et al. Scanned Probe Microscopy of Electronic Transport in Carbon Nanotubes. *Phys Rev Lett* 2000;84:6082–5.
- [70] Tans SJ, Devoret MH, Dai H, Thess A, Smalley RE, Geerligs L, et al. Individual single-wall carbon nanotubes as quantum wires. *Nature* 1997;386:474–7.
- [71] White CT, Todorov TN. Carbon nanotubes as long ballistic conductors. *Nature* 1998;393:240–2.
- [72] Javey A, Guo J, Wang Q, Lundstrom M, Dai H. Ballistic carbon nanotube field-effect transistors. *Nature* 2003;424:654–7.
- [73] Zhang Z, Liang X, Wang S, Yao K, Hu Y, Zhu Y, et al. Doping-Free Fabrication of Carbon Nanotube Based Ballistic CMOS Devices and Circuits. *Nano Lett* 2007;7:3603–7. <https://doi.org/10.1021/nl0717107>.
- [74] Frank S, Poncharal P, Wang ZL, Heer WA De. Carbon Nanotube Quantum Resistors. *Science (1979)* 1998;280:1744–6.

- [75] Berger C, Yi Y, Wang ZL, De Heer WA. Multiwalled carbon nanotubes are ballistic conductors at room temperature. *Applied Physics A* 2002;74:363–5. <https://doi.org/10.1007/s003390201279>.
- [76] Li HJ, Lu WG, Li JJ, Bai XD, Gu CZ. Multichannel Ballistic Transport in Multiwall Carbon Nanotubes. *Phys Rev Lett* 2005;95:086601. <https://doi.org/10.1103/PhysRevLett.95.086601>.
- [77] Poncharal P, Berger C, Yi Y, Wang ZL, De Heer WA. Room Temperature Ballistic Conduction in Carbon Nanotubes. *Journal of Physical Chemistry B* 2002;106:12104–18. <https://doi.org/10.1021/jp021271u>.
- [78] Langer L, Bayot V, Grivei E, Issi J-P, Heremans JP, Olk CH, et al. Quantum Transport in a Multiwalled Carbon Nanotube. *Phys Rev Lett* 1996;76:479–82.
- [79] Avouris P, Chen Z, Perebeinos V. Carbon-based electronics. *Nat Nanotechnol* 2007;2:605–15. <https://doi.org/10.1038/nnano.2007.300>.
- [80] Kaiser AB. Electronic transport properties of conducting polymers and carbon nanotubes. *Reports on Progress in Physics* 2001;64:1–49.
- [81] Han S, Chand A, Araby S, Cai R, Chen S, Kang H, et al. Thermally and electrically conductive multifunctional sensor based on epoxy/graphene composite. *Nanotechnology* 2020;31. <https://doi.org/10.1088/1361-6528/ab5042>.
- [82] Kim YJ, Cha JY, Ham H, Huh H, So DS, Kang I. Preparation of piezoresistive nano smart hybrid material based on graphene. *Current Applied Physics*, vol. 11, 2011. <https://doi.org/10.1016/j.cap.2010.11.022>.
- [83] Skákalová V, Kaiser AB, Woo YS, Roth S. Electronic transport in carbon nanotubes: From individual nanotubes to thin and thick networks. *Phys Rev B* 2006;74:085403. <https://doi.org/10.1103/PhysRevB.74.085403>.
- [84] Bauhofer W, Kovacs JZ. A review and analysis of electrical percolation in carbon nanotube polymer composites. *Compos Sci Technol* 2009;69:1486–98. <https://doi.org/10.1016/j.compscitech.2008.06.018>.
- [85] Gallo GJ, Thostenson ET. Electrical characterization and modeling of carbon nanotube and carbon fiber self-sensing composites for enhanced sensing of microcracks. *Mater Today Commun* 2015;3:17–26. <https://doi.org/10.1016/j.mtcomm.2015.01.009>.
- [86] Gao L, Chou TW, Thostenson ET, Zhang Z, Coulaud M. In situ sensing of impact damage in epoxy/glass fiber composites using percolating carbon nanotube networks. *Carbon N Y* 2011;49:3382–5. <https://doi.org/10.1016/j.carbon.2011.04.003>.

- [87] Kane CL, Mele EJ, Lee RS, Fischer JE, Petit P, Dai H. Temperature-dependent resistivity of single-wall carbon nanotubes. *Europhys Lett* 1998;41:683–8.
- [88] Garcia EJ, Wardle BL, John Hart A. Joining prepreg composite interfaces with aligned carbon nanotubes. *Compos Part A Appl Sci Manuf* 2008;39:1065–70. <https://doi.org/10.1016/j.compositesa.2008.03.011>.
- [89] Conway H, Gouldstone C. Vertically aligned carbon nanotubes as interlaminar reinforcement in carbon fiber composite laminates. *AIAA Scitech 2019 Forum* 2019:1–6. <https://doi.org/10.2514/6.2019-1764>.
- [90] Guzman de Villoria R, Hallander P, Ydrefors L, Nordin P, Wardle BL. In-plane strength enhancement of laminated composites via aligned carbon nanotube interlaminar reinforcement. *Compos Sci Technol* 2016;133:33–9. <https://doi.org/10.1016/j.compscitech.2016.07.006>.
- [91] Kopp R, Ni X, Nordin P, Hallander P, Selegård L, Wardle BL. Hygrothermal progressive damage in open-hole compression of composite laminates with aligned carbon nanotube interlaminar reinforcement studied by X-ray micro-computed tomography. *Compos B Eng* 2024;278. <https://doi.org/10.1016/j.compositesb.2024.111391>.
- [92] Tao Y, Zhang R, Hu X, Ou Y, Ren M, Sun J, et al. A comprehensive review on fiber-based self-sensing polymer composites for in situ structural health monitoring. *Adv Compos Hybrid Mater* 2025;8. <https://doi.org/10.1007/s42114-025-01413-y>.
- [93] Kinet D, Mégret P, Goossen KW, Qiu L, Heider D, Caucheteur C. Fiber Bragg grating sensors toward structural health monitoring in composite materials: Challenges and solutions. *Sensors (Switzerland)* 2014;14:7394–419. <https://doi.org/10.3390/s140407394>.
- [94] Di Sante R, Donati L. Strain monitoring with embedded Fiber Bragg Gratings in advanced composite structures for nautical applications. *Measurement (Lond)* 2013;46:2118–26. <https://doi.org/10.1016/j.measurement.2013.03.009>.
- [95] Kikuchi M, Ogasawara T, Fujii S, Takeda S ichi. Application of machine learning for improved accuracy of simultaneous temperature and strain measurements of carbon fiber-reinforced plastic laminates using an embedded tilted fiber Bragg grating sensor. *Compos Part A Appl Sci Manuf* 2022;161. <https://doi.org/10.1016/j.compositesa.2022.107108>.
- [96] Huang S, Zhang J, Ke Y, Gu B, Sun B. In-situ monitoring of carbon fiber/epoxy composite with FBG sensors under curing and thermal cycling conditions. *Composites Communications* 2024;47. <https://doi.org/10.1016/j.coco.2024.101875>.

- [97] Mulle M, Collombet F, Olivier P, Grunevald Y-H. Assessment of cure residual strains through the thickness of carbon – epoxy laminates using FBGs, Part I : Elementary specimen. *Composites Part A* 2009;40:94–104. <https://doi.org/10.1016/j.compositesa.2008.10.008>.
- [98] Mulle M, Collombet F, Olivier P, Zitoune R, Huchette C, Laurin F, et al. Assessment of cure-residual strains through the thickness of carbon – epoxy laminates using FBGs Part II : Technological specimen. *Composites Part A* 2009;40:1534–44. <https://doi.org/10.1016/j.compositesa.2009.06.013>.